Received: Added at production | Revised: Added at production | Accepted: Added at production

DOI: xxx/xxxx

ARTICLE TYPE

Error Estimates for Golub–Kahan Bidiagonalization with Tikhonov Regularization for Ill–posed Operator Equations

A. Alqahtani[1,2] | R. Ramlau*[3] | L. Reichel[2]

[1]Department of Mathematics, King Khalid University, Abha, Saudi Arabia
[2]Department of Mathematical Sciences, Kent State University, Kent, OH, USA
[3]Industrial Mathematics Institute, Johannes Kepler University, and Johann Radon Institute for Computational and Applied Mathematics, Austrian Academy of Sciences, Linz, Austria

Correspondence
*Ronny Ramlau, via Altenberger Str. 69, A-4040 Linz, Austria. Email: ronny.ramlau@ricam.oeaw.ac.at

Present Address
Present address

Abstract

Linear ill-posed operator equations arise in various areas of science and engineering. The presence of errors in the operator and the data often makes the computation of an accurate approximate solution difficult. In this paper, we compute an approximate solution of an ill-posed operator equation by first determining an approximation of the operators of generally fairly small dimension by carrying out a few steps of a continuous version of the Golub–Kahan bidiagonalization (GKB) process to the noisy operator. Then Tikhonov regularization is applied to the low-dimensional problem so obtained and the regularization parameter is determined by solving a low-dimensional nonlinear equation. The effect of the errors incurred in each step of the solution process is analyzed. Computed examples illustrate the theory presented.

KEYWORDS:
ill-posed problem, inverse problem, Golub–Kahan bidiagonalization, Tikhonov regularization

1 | INTRODUCTION

Let $\mathcal{A} : \mathcal{X} \to \mathcal{Y}$ be an injective linear operator between the Hilbert spaces $\mathcal{X}$ and $\mathcal{Y}$ with norms $\|\cdot\|_{\mathcal{X}}$ and $\|\cdot\|_{\mathcal{Y}}$, respectively, and let $\mathcal{R}(\mathcal{A})$ denote the range of $\mathcal{A}$. Then the equation

$$\mathcal{A}x = y \tag{1.1}$$

has a unique solution $x \in \mathcal{X}$ for every $y \in \mathcal{R}(\mathcal{A})$. Thus, we can define an inverse of $\mathcal{A}$ for $y \in \mathcal{R}(\mathcal{A})$, which we denote by $\mathcal{A}^{-1}$. We are interested in the situation when the solution of (1.1), which we denote by x_{exact}, does not depend continuously on the right-hand side y, i.e., when the inverse operator $\mathcal{A}^{-1}$ is not bounded. Then the computation of the solution of (1.1) is an ill-posed problem.

In many ill-posed problems that arise in applications in physics, technology, and various branches of science, the operator $\mathcal{A}$ and the right-hand side function y in (1.1) are not available. Instead, only an approximation $\mathcal{A}_h$, which we also assume to be injective, of $\mathcal{A}$ and an error-contaminated approximation $y^\delta \in \mathcal{Y}$ of y are known, where $\mathcal{A}_h$ and y^δ satisfy

$$\|\mathcal{A} - \mathcal{A}_h\| \le h, \qquad \|y - y^\delta\|_{\mathcal{Y}} \le \delta, \tag{1.2}$$

for some scalars $h > 0$ and $\delta > 0$. Here $\|\cdot\|$ denotes the operator norm induced by the norms $\|\cdot\|_{\mathcal{X}}$ and $\|\cdot\|_{\mathcal{Y}}$, i.e.,

$$\|A\| = \sup_{x \in \mathcal{X}\setminus\{0\}} \frac{\|Ax\|_{\mathcal{Y}}}{\|x\|_{\mathcal{X}}}.$$

We will let $\mathcal{X}$ and $\mathcal{Y}$ be L_2-spaces. Then $\|A\|$ is the largest singular value of A.

Our task is to determine an approximation of x_{exact} by computing an approximate solution of the available equation

$$\mathcal{A}_h x = y^\delta. \tag{1.3}$$

The perturbed right-hand side y^δ might not be in $\mathcal{R}(\mathcal{A}_h)$; then equation (1.3) does not have a solution. It follows that the computation of a solution of (1.3) also might be an ill-posed problem. Moreover, even when $y^\delta \in \mathcal{R}(\mathcal{A}_h)$, the solution x^δ of (1.3) might not be a meaningful approximation of the solution x_{exact} of (1.1) since $\mathcal{A}_h$ might not have a bounded inverse.

The solution of inverse problems with an inexact operator and a noisy right-hand side has been widely discussed in the literature; see, e.g.,[4, 18, 21]. The approach of the present paper differs from previous investigations in that it focuses on Golub–Kahan bidiagonalization. Our analysis is inspired by the work of Neubauer[21], who approximates the operator $\mathcal{A}_h$ in a fairly general finite-dimensional subspace. We are interested in discretizing $\mathcal{A}_h$ with the aid of Golub–Kahan bidiagonalization due to the fact that typically only very few bidiagonalization steps, and therefore a subspace of low dimension, are required to determine a suitable approximation of x_{exact}. This makes this solution approach inexpensive. Illustrations of the performance of Golub–Kahan bidiagonalization when $\mathcal{A}$ is a finite-dimensional matrix and y^δ a finite-dimensional vector can be found, e.g., in[5].

Due to the ill-posed nature of problem (1.3), it is necessary to apply regularization, i.e., the operator $\mathcal{A}_h$ in (1.3) is replaced by an operator $\mathcal{A}_{\text{reg}}^\delta : \mathcal{X} \to \mathcal{Y}$ that approximates $\mathcal{A}_h$ in some sense and has a bounded inverse on $\mathcal{X}$. Therefore, instead of solving equation (1.3), one solves the regularized equation

$$\mathcal{A}_{\text{reg}}^\delta x = y^\delta. \tag{1.4}$$

It is desirable to choose the regularized operator $\mathcal{A}_{\text{reg}}^\delta$ so that the solution $x_{\text{reg}}^{\delta,h}$ of (1.4) is a meaningful approximation of the solution x_{exact} of equation (1.1) with unknown operator and right-hand side function.

One of the most commonly used regularization methods is Tikhonov regularization, which approximates x_{exact} by the unique minimizer $x_\mu^{\delta,h}$ of the functional

$$J_\mu(x) := \|\mathcal{A}_h x - y^\delta\|_{\mathcal{Y}}^2 + \mu\|x\|_{\mathcal{X}}^2, \tag{1.5}$$

where $\mu > 0$ is a regularization parameter. Then $(\mathcal{A}_{\text{reg}}^\delta)^{-1} = (\mathcal{A}_h^*\mathcal{A}_h + \mu I)^{-1}\mathcal{A}_h^*$, where $\mathcal{A}_h^*$ denotes the adjoint of $\mathcal{A}_h$, and I is the identity. Numerically, one determines an approximate solution of (1.5) by minimizing J_μ over some m-dimensional subspace $\mathcal{V}_m$, $1 \le m < \infty$, of $\mathcal{X}$. We denote the approximate solution of (1.5) so obtained by $x_{\mu,m}^{\delta,h}$. The choice of a suitable value of the regularization parameter μ is important. This parameter determines how sensitive the computed approximate solution $x_{\mu,m}^{\delta,h}$ of (1.5) is to perturbations in y and how close $x_{\mu,m}^{\delta,h}$ is to the solution x_{exact} of (1.1). Ideally, one would like to choose $\mu = \mu(m, \delta, h)$ so that the minimizer $x_{\mu,m}^{\delta,h}$ of J_μ over $\mathcal{V}_m$ satisfies

$$\lim_{\substack{m\to\infty \\ \delta,\, h\to 0}} x_{\mu,m}^{\delta,h} = x_{\text{exact}},$$

and that the rate of convergence is high.

There are several strategies for determining a suitable value of μ, including the discrepancy principle, generalized cross validation, and the L-curve criterion; see, e.g.,[7–9, 12, 13, 16, 17, 19, 24] for recent discussions on these and other methods. We will determine the regularization parameter $\mu > 0$ by an approach closely related to the one described by Neubauer[21]. It allows discretization and other errors both in the operator and right-hand side function. We will carry out an analogous analysis for the situation when $\mathcal{A}_h$ is discretized by a continuous version of the partial Golub–Kahan bidiagonalization (GKB) process. Application of a few steps of this process gives a finite-dimensional approximation of the operator $\mathcal{A}_h$. We replace $\mathcal{A}_h$ in (1.3) by this approximation, and compute an approximate solution of the operator equation so obtained with the aid of Tikhonov regularization. This replacement reduces the computational cost of Tikhonov regularization. We will discuss the effect of this replacement on the computed solution, as well as the effect of the errors in the operator $\mathcal{A}_h$ and in the right-hand side function y^δ. Another approach for determining a low-rank approximation of the operator $\mathcal{A}_h$ by applying the Arnoldi process instead of the GKB process has been discussed in[23]. This approach is quite different from the one of the present paper and is based on results by Natterer[20].

This paper is organized as follows. Section 2 discusses the application of the GKB process to the operator $\mathcal{A}_h$, which gives orthonormal bases for finite-dimensional (and usually low-dimensional) subspaces of $\mathcal{X}$ and $\mathcal{Y}$. These bases allow us to define an approximation of finite (and usually low) rank of the operator $\mathcal{A}_h$ in (1.3). In Section 3, we discuss the effect of the error in this approximation of $\mathcal{A}_h$. A few computed examples in Section 4, some of which using the MATLAB package Chebfun, which simulates operators and functions, illustrate the theory. Concluding remarks can be found in Section 5.

2 | GOLUB–KAHAN BIDIAGONALIZATION

This section describes the Golub–Kahan bidiagonalization (GKB) process for linear operators. An analogous discussion is presented by Karimi and Jozi[15]. Before describing the GKB process, we need the following definition.

Definition 1. Let $\mathcal{X}$ and $\mathcal{Y}$ be Hilbert spaces and let $\mathcal{A} : \mathcal{X} \to \mathcal{Y}$ be a linear operator. Let $\boldsymbol{z} = [z_1, z_2, \dots, z_m]^T \in \mathbb{R}^m$, $C \in \mathbb{R}^{m\times m}$ and $V_m = [v_1, v_2, \dots, v_m]$, where the $v_i \in \mathcal{X}$, $i = 1, 2, \dots, m$, are orthonormal functions to be specified below. Define

(i) $V_m\boldsymbol{z} := \sum_{i=1}^m z_i v_i \in \mathcal{X}$.

(ii) $V_m C := [V_m C(:, 1), V_m C(:, 2), \dots, V_m C(:, m)] \in \mathcal{X}^m$, where $C(:, i) \in \mathbb{R}^m$ denotes the ith column of the matrix C.

(iii) $\mathcal{A}V_m := [\mathcal{A}v_1, \mathcal{A}v_2, \dots, \mathcal{A}v_m] \in \mathcal{Y}^m$.

Here $\mathcal{X}^m$ and $\mathcal{Y}^m$ denote m-dimensional subspaces of elements in $\mathcal{X}$ and $\mathcal{Y}$, respectively. We also will need the inner products $\langle\cdot,\cdot\rangle_{\mathcal{X}}$ and $\langle\cdot,\cdot\rangle_{\mathcal{Y}}$ of functions in $\mathcal{X}$ and $\mathcal{Y}$, respectively.

Application of $m + 1$ steps of the GKB process (see Algorithm 1 below) to the operator $\mathcal{A}_h$ with initial function $\mathcal{A}_h\mathcal{A}_h^* y^\delta$ gives the decompositions

$$\mathcal{A}_h V_m = U_{m+1} C_{m+1,m}, \qquad \mathcal{A}_h^* U_m = V_m C_{m,m}^*, \tag{2.1}$$

where the entries of $V_m = [v_1, v_2, \dots, v_m] \in \mathcal{X}^m$ and $U_{m+1} = [u_1, u_2, \dots, u_{m+1}] \in \mathcal{Y}^{m+1}$ are orthonormal functions in $\mathcal{X}$ and $\mathcal{Y}$, respectively, i.e.,

$$\langle v_i, v_j\rangle_{\mathcal{X}} = \langle u_i, u_j\rangle_{\mathcal{Y}} = \begin{cases} 1, & i = j, \\ 0, & i \neq j, \end{cases} \qquad \text{for } i, j = 1, 2, \dots,$$

with $u_1 = \mathcal{A}_h\mathcal{A}_h^* y^\delta / \|\mathcal{A}_h\mathcal{A}_h^* y^\delta\|_{\mathcal{Y}}$. Moreover,

$$C_{m+1,m} = \begin{bmatrix} \alpha_1 & & & \\ \beta_2 & \alpha_2 & & \\ & \ddots & \ddots & \\ & & \beta_m & \alpha_m \\ & & & \beta_{m+1} \end{bmatrix} \in \mathbb{R}^{(m+1)\times m}$$

is a lower bidiagonal matrix, and $C_{m,m} \in \mathbb{R}^{m\times m}$ denotes its leading $m \times m$ submatrix. The matrix $C_{m,m}^*$ denotes the transpose of $C_{m,m}$. Note that the matrix $C_{m+1,m}^* C_{m+1,m}$ is positive definite because it is an orthogonal section of the positive definite operator $\mathcal{A}_h^*\mathcal{A}_h$. We remark that the initial function $\mathcal{A}_h\mathcal{A}_h^* y^\delta$ is not an analogue of the standard choice of initial vector often used in a linear algebra context; see[22]. Our reason for this choice of initial function is that we would like it to be in the range of $\mathcal{A}_h$. Algorithm 1 describes the GKB process under the assumption that breakdown of the recursion relations does not occur. We comment on how to handle breakdown at the end of this section. The algorithm also determines the function v_{m+1} which is required in the decomposition (3.6) below.

Algorithm 1 The Golub–Kahan bidiagonalization (GKB) process.

Input: : Linear operator $\mathcal{A}_h$, the right-hand side $y^\delta \neq 0$, number of steps $m + 1 \geq 1$
Initialize: $\beta_1 = \|\mathcal{A}_h\mathcal{A}_h^* y^\delta\|_{\mathcal{Y}}$, $u_1 = \mathcal{A}_h\mathcal{A}_h^* y^\delta/\beta_1$, $v = \mathcal{A}_h^* u_1$, $\alpha_1 = \|v\|_{\mathcal{X}}$, $v_1 = v/\alpha_1$
For $j = 2, \dots, m + 1$
  $u = \mathcal{A}_h v_{j-1} - \alpha_{j-1} u_{j-1}$
  $\beta_j = \|u\|_{\mathcal{Y}}$
  $u_j = u/\beta_j$
  $v = \mathcal{A}_h^* u_j - \beta_j v_{j-1}$
  $\alpha_j = \|v\|_{\mathcal{X}}$
  $v_j = v/\alpha_j$
EndFor
Output: Golub–Kahan decomposition (2.1)

It is easy to see that the functions $\{u_j\}_{j=1}^{m+1}$ and $\{v_j\}_{j=1}^{m+1}$ generated by Algorithm 1 form orthonormal bases for the Krylov subspaces

$$\mathcal{K}_{m+1}(\mathcal{A}_h\mathcal{A}_h^*, \mathcal{A}_h\mathcal{A}_h^* y^\delta) = \text{span}\{\mathcal{A}_h\mathcal{A}_h^* y^\delta, \dots, (\mathcal{A}_h\mathcal{A}_h^*)^{m+1} y^\delta\},$$
$$\mathcal{K}_{m+1}(\mathcal{A}_h^*\mathcal{A}_h, (\mathcal{A}_h^*\mathcal{A}_h)\mathcal{A}_h^* y^\delta) = \text{span}\{(\mathcal{A}_h^*\mathcal{A}_h)\mathcal{A}_h^* y^\delta, \dots, (\mathcal{A}_h^*\mathcal{A}_h)^{m+1}\mathcal{A}_h^* y^\delta\},$$

respectively; see also[15] for a discussion of the GKB process for operators. For the situation when $\mathcal{A}_h$ is a finite-dimensional matrix, this process is described by Paige and Saunders[22].

We remark that the functions v_j and u_j determined by Algorithm 1 are orthonormal when the computations are carried out in exact arithmetic. However, when the computations are carried out in finite-precision arithmetic, this is typically not the case. We apply reorthogonalization in the computed examples reported in Section 4 to avoid loss of orthogonality.

Algorithm 1 assumes that $m+1$ steps can be carried out without breakdown, i.e., without any of the coefficients $\alpha_1, \alpha_2, \dots, \alpha_{m+1}$ and $\beta_1, \beta_2, \dots, \beta_{m+1}$ vanishing. This is the generic situation. In particular, this implies that y^δ is not allowed to be an eigenfunction of $\mathcal{A}_h\mathcal{A}_h^*$ associated with a zero eigenvalue.

We conclude this section with some comments on the rare event of breakdown of the recursions of Algorithm 1. First consider the case when $\alpha_k > 0$ for $1 \le k < j$ and $\beta_k > 0$ for $2 \le k < j$, but $\beta_j = 0$. Then the decompositions

$$\mathcal{A}_h V_{j-1} = U_{j-1} C_{j-1,j-1}, \qquad \mathcal{A}_h^* U_{j-1} = V_{j-1} C_{j-1,j-1}^*,$$

which are analogous to (2.1) can be computed, but the "next" function u_j cannot be generated by the algorithm. If the above decompositions yield an approximation of x_{exact} of sufficient accuracy, then we are done; otherwise we can let u_j be a fairly arbitrary function that is orthogonal to the available functions $u_1, u_2, \dots, u_{j-1}$, substitute it into the algorithm and continue the computations. In the theory developed below, we rule out this situations because it is very unusual, and it is difficult to show results when the solution subspace contains fairly arbitrary functions.

We now investigate whether breakdown can occur in Algorithm 1 when

$$\alpha_k > 0, \quad 1 \le k < j, \qquad \beta_k > 0, \quad 2 \le k \le j, \qquad \alpha_j = 0.$$

In this case, $\mathcal{A}_h^* u_j = \beta_j v_{j-1}$, and we can compute the decomposition

$$\mathcal{A}_h^* U_j = V_{j-1} C_{j,j-1}^*.$$

Since $\mathcal{A}_h$ is injective, so is $\mathcal{A}_h^*$. Therefore, the space $\{\mathcal{A}_h^* U_j z,\ z \in \mathbb{R}^j\}$ is of dimension j, but the space $\{V_{j-1} C_{j,j-1}^* z,\ z \in \mathbb{R}^j\}$ is of dimension $j-1$. This contradiction shows that $\alpha_j > 0$.

3 | ERROR ESTIMATES

Let us first consider the situation when we just have an error in the operator $\mathcal{A}$, i.e., when $\mathcal{A} \neq \mathcal{A}_h$ and $y = y^\delta$. Let x_μ denote the minimizer of J_μ in (1.5) over $\mathcal{X}$ with y^δ replaced by y, and let x_μ^h denote the corresponding minimizer obtained when $\mathcal{A}$ is replaced by $\mathcal{A}_h$. Thus,

$$x_\mu = (\mathcal{A}^*\mathcal{A} + \mu I)^{-1}\mathcal{A}^* y,$$
$$x_\mu^h = (\mathcal{A}_h^*\mathcal{A}_h + \mu I)^{-1}\mathcal{A}_h^* y.$$

It is known[19] that

$$\|x_\mu - x_\mu^h\|_{\mathcal{X}} \le c \cdot \frac{\|\mathcal{A} - \mathcal{A}_h\|}{\mu}$$

for some constant $c > 0$ independent of μ and h. Assume that $y \in \mathcal{R}(\mathcal{A})$. Then Neubauer[21] (Lemma 2.1) shows that

$$\|x_\mu - x_\mu^h\|_{\mathcal{X}} \le \frac{\|\mathcal{A} - \mathcal{A}_h\|}{\sqrt{\mu}} \|x_{\text{exact}}\|_{\mathcal{X}} + \frac{\|Q_h(I - Q)y\|_{\mathcal{Y}}}{2\sqrt{\mu}}, \tag{3.1}$$

where Q and Q_h denote the orthogonal projectors onto $\overline{\mathcal{R}(\mathcal{A})}$ and $\overline{\mathcal{R}(\mathcal{A}_h)}$, respectively.

Remark 1. Assume that

$$\|\mathcal{A} - \mathcal{A}_h\| \le h \quad \text{and} \quad \|Q_h(I - Q)y\|_{\mathcal{Y}} \le h$$

for some scalar $h > 0$. It can be shown that, if

$$h/\sqrt{\mu} \to 0 \quad \text{for } \mu \to 0,$$

then

$$x_\mu^h \to x_{\text{exact}} \quad \text{for } \mu \to 0 \quad \text{and} \quad h \to 0;$$

see[26] Chapter III.

Since $\mathcal{A}^*$ is injective, $\overline{\mathcal{R}(\mathcal{A})} = \mathcal{Y}$ and $Q = I$, where I denotes the identity operator. Therefore, $Q_h(I - Q)y = 0$ and the bound (3.1) simplifies to

$$\|x_\mu - x_\mu^h\|_{\mathcal{X}} \leq \frac{\|\mathcal{A} - \mathcal{A}_h\|}{\sqrt{\mu}} \|x_{\text{exact}}\|_{\mathcal{X}}.$$

We turn to the situation when the right-hand side function is error-contaminated and assume that $y^\delta \in \mathcal{Y}$. In the numerical computations, we project the operator $\mathcal{A}_h$ into the finite-dimensional subspace

$$\widetilde{\mathcal{W}}_{m+1} = \mathcal{R}(U_{m+1}) = \mathcal{K}_{m+1}(\mathcal{A}_h\mathcal{A}_h^*, \mathcal{A}_h\mathcal{A}_h^* y^\delta) \tag{3.2}$$

for a suitable $m > 0$.

The adjoint U_{m+1}^* of U_{m+1} is applied to functions $z \in \mathcal{Y}$ as

$$U_{m+1}^* z = \left[\langle z, u_1\rangle, \langle z, u_2\rangle, \ldots, \left\langle z, u_{m+1}\right\rangle\right]^T.$$

Due to the orthonormality of the functions $u_1, u_2, \ldots, u_{m+1}$, the operator $U_{m+1}^* U_{m+1}$ is the identity in $\widetilde{\mathcal{W}}_{m+1}$ and

$$\widetilde{Q}_{m+1} = U_{m+1}U_{m+1}^* \tag{3.3}$$

is an orthogonal projector onto $\widetilde{\mathcal{W}}_{m+1}$. This projector is determined by applying $m + 1$ steps of the GKB process to the operator $\mathcal{A}_h$ with initial function $\mathcal{A}_h\mathcal{A}_h^* y^\delta$.

Define the projector $\widetilde{P}_{m+1} := V_{m+1}V_{m+1}^*$. We will approximate x_{exact} by

$$x_{\mu,m+1}^{h,\delta} = (\mathcal{A}_{h,m+1}^*\mathcal{A}_{h,m+1} + \mu I)^{-1}\mathcal{A}_{h,m+1}^* y^\delta, \qquad \mathcal{A}_{h,m+1} = \widetilde{Q}_{m+1}\mathcal{A}_h\widetilde{P}_{m+1} \tag{3.4}$$

for some $\mu > 0$. Thus, $\mathcal{A}_{h,m+1}$ is a projection of $\mathcal{A}_h$ that is determined by $\widetilde{Q}_{m+1}$and $\widetilde{P}_{m+1}$.

Assume that infinitely many steps of the Golub–Kahan bidiagonalization process can be applied to the operator $\mathcal{A}_h$ with initial function $\mathcal{A}_h\mathcal{A}_h^* y^\delta$ without breakdown. This results in infinite vectors $U = [u_1, u_2, \ldots\ ]$ and $V = [v_1, v_2, \ldots\ ]$ with orthonormal function elements and an infinite lower bidiagonal matrix C; see[15]. We will determine (approximate) solutions of (1.1) in subsets of the space $\mathcal{R}(V)$ and, therefore, consider the restriction of $\mathcal{A}_h$ to this space. We have analogously to (2.1) the decompositions

$$\mathcal{A}_h V = UC, \qquad \mathcal{A}_h^* U = V\,C^*. \tag{3.5}$$

This is the infinite-dimensional analogue of (2.1).

Introduce the orthogonal projector $\widetilde{P} = VV^*$ and consider the projection of $\mathcal{A}_h\widetilde{P}$ onto the space (3.2). Then

$$\begin{aligned}\widetilde{Q}_{m+1}\mathcal{A}_h\widetilde{P} &= \widetilde{Q}_{m+1}(\mathcal{A}_h V)V^* \\ &= U_{m+1}U_{m+1}^*(UC)V^* \\ &= U_{m+1}[C_{m+1,m+1}, O]V^* \\ &= U_{m+1}C_{m+1,m+1}V_{m+1}^*,\end{aligned}$$

where $C_{m+1,m+1}$ is the leading $(m + 1) \times (m + 1)$ principal submatrix of the infinite bidiagonal matrix C in (3.5) and the zero matrix O has $m + 1$ rows and infitiely many columns. We will approximate $\mathcal{A}_h$ by

$$\mathcal{A}_{h,m+1} = U_{m+1}C_{m+1,m+1}V_{m+1}^*. \tag{3.6}$$

The following result is both a generalization and specialization of Alqahtani et al.[1] (Corollary 3); it is a generalization because infinite-dimensional operators are considered, and it is a specialization because tridiagonal matrices with scalar entries are regarded.

Theorem 1. Let $\{\lambda_i; w_i\}_{i=1}^\infty$ be an eigensystem of the self-adjoint compact operator $\mathcal{A}_h\widetilde{P}\mathcal{A}_h^*$. Assume that the eigenvalues are ordered so that $\lambda_i \geq \lambda_{i+1} \geq 0$ for all $i \geq 1$, and let the eigenfunctions w_i be orthonormal. Assume that the Golub–Kahan bidiagonalization process applied to $\mathcal{A}_h$ with initial function $\mathcal{A}_h\mathcal{A}_h^* y^\delta$ can be carried out infinitely many steps without

breakdown, and let the α_i and β_i be the diagonal and subdiagonal entries, respectively, of the (infinite) bidiagonal matrix $\boldsymbol{C}$ in (3.5). It follows from Algorithm 1 that these entries are positive. Then

$$\prod_{i=1}^{m+1} \alpha_i \beta_{i+1} \leq \prod_{i=1}^{m} \lambda_i, \qquad m = 1, 2, \dots \ . \tag{3.7}$$

Proof. Let $\mathcal{A}_h \widetilde{P} \mathcal{A}_h^* = S \Lambda S^*$ denote the spectral factorization, where $\Lambda = \mathrm{diag}[\lambda_1, \lambda_2, \dots\ ]$ and S is a unitary operator. Introduce the monic polynomial $p_m(t) = \prod_{i=1}^{m}(t - \lambda_i)$ with $1 \leq m < \infty$. The eigenvalues λ_j are nonnegative, since they are the square of the singular values of $\mathcal{A}_h V$. Therefore,

$$\|p_m(\mathcal{A}_h \widetilde{P} \mathcal{A}_h^*)\| = \|p_m(\Lambda)\| = \sup_{j \geq m+1} |p_m(\lambda_j)| \leq |p_m(0)| = \prod_{i=1}^{m} \lambda_i.$$

Hence,

$$\|p_m(\mathcal{A}_h \widetilde{P} \mathcal{A}_h^*) \mathcal{A}_h \mathcal{A}_h^* y^\delta\|_{\mathcal{Y}} \leq \|\mathcal{A}_h \mathcal{A}_h^* y^\delta\|_{\mathcal{Y}} \prod_{i=1}^{m} \lambda_i. \tag{3.8}$$

Application of infinitely many steps of the Golub–Kahan bidiagonalization process to the operator $\mathcal{A}_h$ with initial function $\mathcal{A}_h \mathcal{A}_h^* y^\delta$ gives (3.5) with $u_1 = \mathcal{A}_h \mathcal{A}_h^* y^\delta / \|\mathcal{A}_h \mathcal{A}_h^* y^\delta\|_{\mathcal{Y}}$. We obtain from (3.5) that

$$\mathcal{A}_h \widetilde{P} \mathcal{A}_h^* = U T U^*, \tag{3.9}$$

where $T = [t_{ij}]_{i,j=1}^{\infty} := CC^*$ is an infinite symmetric tridiagonal matrix with diagonal entries $t_{ii} = \alpha_i^2 + \beta_i^2$, $i = 1, 2, \dots$, with $\beta_1 = 0$, and subdiagonal entries $t_{i+1,i} = \beta_{i+1}\alpha_i$, $i = 1, 2, \dots$. We have

$$p_m(\mathcal{A}_h \widetilde{P} \mathcal{A}_h^*) \mathcal{A}_h \mathcal{A}_h^* y^\delta = U p_m(T) U^* \mathcal{A}_h \mathcal{A}_h^* y^\delta = U p_m(T) e_1 \|\mathcal{A}_h \mathcal{A}_h^* y^\delta\|_{\mathcal{Y}}.$$

Here and in the following, $e_j = [0, \dots, 0, 1, 0, 0, \dots\ ]^T$ denotes the (infinite) jth axis vector and $\|\cdot\|_2$ denotes the ℓ_2-norm. The next inequality follows by direct computation,

$$\|p_m(\mathcal{A}_h \widetilde{P} \mathcal{A}_h^*) \mathcal{A}_h \mathcal{A}_h^* y^\delta\|_{\mathcal{Y}} = \|p_m(T) e_1\|_2 \|\mathcal{A}_h \mathcal{A}_h^* y^\delta\|_{\mathcal{Y}} \geq \|\mathcal{A}_h \mathcal{A}_h^* y^\delta\|_{\mathcal{Y}} \|e_{m+1}^T p_m(T) e_1\|_2. \tag{3.10}$$

We will show by induction over $m \geq 1$ that

$$e_{m+1}^T p_m(T) e_1 = \prod_{i=1}^{m+1} \alpha_i \beta_{i+1} \tag{3.11}$$

for $m \geq 1$. When $m = 1$, equation (3.11) becomes

$$e_2^T p_m(T) e_1 = [\alpha_1\beta_2, (\alpha_2^2 + \beta_2^2) - \lambda_1, \alpha_2\beta_3, 0, 0, \dots\ ] e_1 = \alpha_1\beta_2.$$

Assume that equation (3.11) holds for $m \geq 2$. We would like to show that (3.11) is valid for $m + 1$. We have

$$\begin{aligned} e_{m+2}^T p_{m+1}(T) e_1 &= e_{m+2}^T (T - \lambda_{m+1} I) p_m(T) e_1 \\ &= (\alpha_{m+2}\beta_{m+3} e_{m+1}^T + ((\alpha_{m+2}^2 + \beta_{m+2}^2) - \lambda_{m+1}) e_{m+2}^T + \alpha_{m+3}\beta_{m+4} e_{m+3}^T) p_m(T) e_1. \end{aligned}$$

Since the operator $p_m(T)$ is $(2m + 1)$-banded, it follows that

$$e_{m+2}^T p_{m+1}(T) e_1 = \alpha_{m+2}\beta_{m+3} e_{m+1}^T p_m(T) e_1.$$

Applying the induction hypothesis, we obtain

$$e_{m+2}^T p_{m+1}(T) e_1 = \alpha_{m+2}\beta_{m+3} \prod_{i=1}^{m+1} \alpha_i \beta_{i+1} = \prod_{i=1}^{m+2} \alpha_i \beta_{i+1}.$$

Thus, the relation (3.11) holds. Substituting (3.11) into (3.10), and combining with (3.8), shows the theorem. □

Figure 1 displays, in logarithmic scale, the values taken by each side of inequality (3.7) with the number of iteration, m, ranging from 1 to 10. The graphs show that the product $\prod_{i=1}^{m+1} \alpha_i \beta_{i+1}$ converges to zero much faster than the product $\prod_{i=1}^{m} \lambda_i$ as m increases. The operators are integral operators of the first kind defined in Section 4.

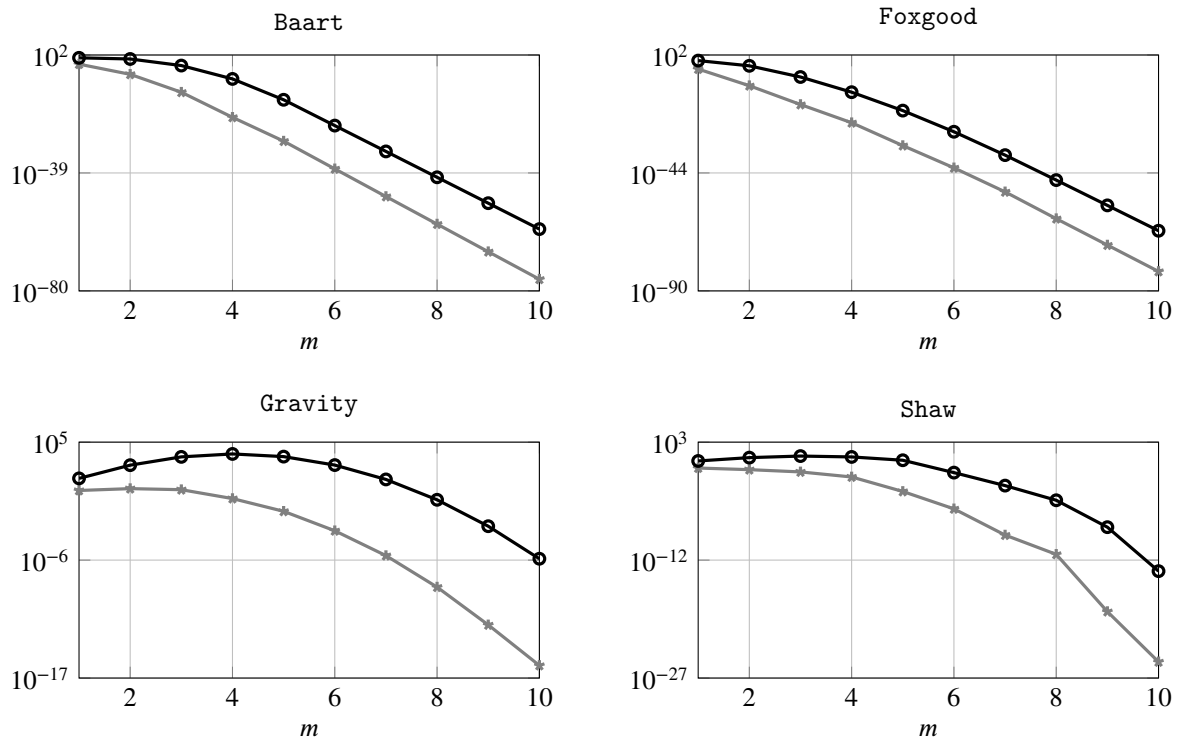

FIGURE 1 Behavior of the bound (3.7) with respect to the iteration index m for `Baart`, `Foxgood`, `Gravity`, and `Shaw` integral equations of the first kind. These integral equations are described in Section 4. The left-hand side of inequality (3.7) is represented by gray stars and the right-hand side is represented by black circles.

Theorem 2. Let $\mathcal{A}_h$ be a compact operator and assume that infinitely many steps of the Golub–Kahan bidiagonalization process can be applied to this operator with initial function $\mathcal{A}_h\mathcal{A}_h^* y^\delta$ without breakdown. Let the identity (3.5) hold and let $\mathcal{A}_{h,m+1}$ be given by (3.6). Furthermore, assume that, for all $j \geq 1$,

$$\alpha_{j+1}\beta_{j+2} \leq \rho \min_{1\leq i\leq j} \alpha_i\beta_{i+1}, \tag{3.12}$$

$$\alpha_{j+1}^2 + \beta_{j+1}^2 \leq \rho \min_{1\leq i\leq j} (\alpha_i^2 + \beta_i^2), \tag{3.13}$$

for some constant ρ independent of j. Here the α_i and β_i are the nontrivial entries of the lower bidiagonal matrix C in (3.5). Then the bound $\gamma_{m+1} > 0$ in

$$\|\mathcal{A}_h\widetilde{P} - \mathcal{A}_{h,m+1}\| \leq \gamma_{m+1} \tag{3.14}$$

can be chosen arbitrarily small by letting m be sufficiently large.

Proof. Consider the infinite tridiagonal matrix $T = CC^*$ of the proof of Theorem 1; see (3.9). It has diagonal entries $t_{ii} = \alpha_i^2+\beta_i^2$, $i = 1, 2, \dots$, with $\beta_1 = 0$, and subdiagonal entries $t_{i+1,i} = \beta_{i+1}\alpha_i$, $i = 1, 2, \dots$. It follows from (3.7) that the product of the subdiagonal entries $t_{i+1,i}$ of T converges to zero as the number of factors, $t_{i+1,i}$, increases. The requirment (3.12) secures that the subdiagonal entries $t_{i+1,i}$ converge to zero as i increases. Let $\varepsilon > 0$ be an arbitrary (small) constant. Then there is an integer m_ε, depending on ε, such that $t_{i-1,i} \leq \varepsilon$ for all $i \geq m_\varepsilon$. In particular, $\lim_{i\to\infty} t_{i-1,i} = 0$.

We turn to the diagonal entries t_{ii} of T. Since $\mathcal{A}_h\mathcal{A}_h^*$ is a compact operator, its eigenvalues cluster at the origin, which is the only cluster point. The matrix T is unitarily similar to the operator $\mathcal{A}_h\widetilde{P}\mathcal{A}_h^*$. Therefore, its eigenvalues also cluster at the origin, and this is the only cluster point. In particular, T has only finitely many, say $\widetilde{m}_\varepsilon$, eigenvalues larger than ε.

We now show that the diagonal entries t_{ii} of T converge to zero as i increases. Assume to the contrary that the t_{ii} are bounded below by $\eta > 0$ for all $i \geq m_\eta$ for some finite $m_\eta \geq 1$. Let $\varepsilon = \eta/3$ and $m = \max\{m_\varepsilon, m_\eta, m\}$. Define the symmetric tridiagonal matrix T_0 by setting all the diagonal and off-diagonal entries t_{ii} and $t_{i+1,i}$ of T to zero for $1 \leq i \leq m + 1$. Then T_0 is a compact operator with all entries of its leading $m + 1$ rows and columns vanishing. Thus, T_0 has $m + 1$ vanishing eigenvalues. The

remaining eigenvalues of T_0 can be bounded with the aid of Gershgorin disks. These eigenvalues are in the set

$$\{z \in \mathbb{C} : \cup_{j=m+2}^{\infty} |z - t_{jj}| \leq t_{j,j-1} + t_{j+1,j}\}. \tag{3.15}$$

The radius of every disk $\{z \in \mathbb{C} : |z - t_{jj}| \leq t_{j,j-1} + t_{j+1,j}\}$ is bounded by $2\varepsilon = \frac{2}{3}\eta$, and the diagonal entries are bounded below by η. Therefore, every nonvanishing eigenvalue λ of T_0 satisfies

$$|\lambda - t_{ii}| \leq \frac{2}{3}\eta,$$

which leads to

$$\eta - \lambda \leq \frac{2}{3}\eta,$$

i.e., $\lambda \geq \eta/3$, Hence, the eigenvalues of T_0 do not cluster at the origin. This contradiction shows that the t_{ii} are not bounded below by a constant strictly larger than zero. The requirement (3.13) secures that $\lim_{i\to\infty} \alpha_i^2 + \beta_i^2 = 0$.

Since both the diagonal and subdiagonal entries of T_0 converge to zero with increasing index number, we may choose the cut-off index m large enough so that

$$t_{i-1,i} + t_{ii} + t_{i+1,i} \leq \gamma_{m+1}^2 \quad \forall i \geq m+1.$$

Application of Gershgorin disks then shows that the largest eigenvalue of T_0 is bounded by γ_{m+1}^2. Introduce the infinite lower bidiagonal matrix

$$C_0 = \begin{bmatrix} \mathrm{O}_m & & & \\ \vdots & & & \\ & \beta_{m+2} & \alpha_{m+2} & \\ & & \beta_{m+3} & \alpha_{m+3} \\ & & & \ddots \quad \ddots \end{bmatrix},$$

where O_m denotes the zero matrix with m columns and infinitely many rows. Then $T_0 = C_0 C_0^*$ and $\|C_0\|_2 = \|T_0\|_2^{1/2} \leq \gamma_{m+1}$. Finally, we obtain from (3.5) and (3.6) that

$$\mathcal{A}_h \widetilde{P} - \mathcal{A}_{h,m+1} = UCV^* - U_{m+1} C_{m+1,m+1} V_{m+1}^* = UC_0 V^*.$$

It follows that

$$\|\mathcal{A}_h \widetilde{P} - \mathcal{A}_{h,m+1}\| = \|C_0\|_2.$$

This shows that the bound (3.14) can be chosen arbitrarily small by letting m be sufficiently large. □

Figure 2 displays the convergence of the diagonal entries t_{ii} and subdiagonal entries $t_{i+1,i}$ of the matrix T in (3.9) to zero as i increases. The matrices T are determined by Fredholm integral equations of the first kind described in Section 4.

Golub–Kahan bidiagonalization determines a basis $\{v_1, v_2, \dots\}$ for the solution subspace. The operator $\mathcal{A}_h$ maps this basis to orthonormal functions $\{u_1, u_2, \dots\}$ in the range of $\mathcal{A}_h$. We will let $\mathcal{Y} = \mathrm{span}\{u_1, u_2, \dots\}$ and, if necessary, replace y in (1.1) by $UU^* y$.

The following proposition establishes that the conditions in Neubauer[21] (Assumption 2.3) are satisfied.

Proposition 1. Assume that the Golub–Kahan bidiagonalization process applied to $\mathcal{A}_h$ with initial function $\mathcal{A}_h \mathcal{A}_h^* y^\delta$ can be carried out infinitely many steps without breakdown and that the representation (3.5) holds. Let $\mathcal{W}_{m+1} = \mathcal{R}(\mathcal{A}_{h,m+1})$ for $m = 0, 1, \dots$. Then with the operators defined as above, we have

$$\mathcal{W}_{m+1} \subset \overline{\mathcal{R}(\mathcal{A}_h \widetilde{P})}, \tag{3.16}$$

$$\mathcal{R}(\widetilde{Q}_{m+1} \mathcal{A}_{h,m+1}) = \mathcal{W}_{m+1}, \tag{3.17}$$

$$\|\widetilde{Q}_{m+1}(\mathcal{A}_h \widetilde{P} - \mathcal{A}_{h,m+1})\| \leq \gamma_{m+1}, \tag{3.18}$$

$$\|\widetilde{Q}_{m+1}(y - y^\delta)\|_{\mathcal{Y}} \leq \delta, \tag{3.19}$$

$$\widetilde{Q}_{m+1} \to I \ \text{ as } \ m \to \infty \quad \text{point-wise in } \mathcal{R}(U). \tag{3.20}$$

Proof. It follows from (3.6) that

$$\mathcal{A}_{h,m+1} \widetilde{P} = U_{m+1} C_{m+1,m+1} V_{m+1}^* = \mathcal{A}_{h,m+1}$$

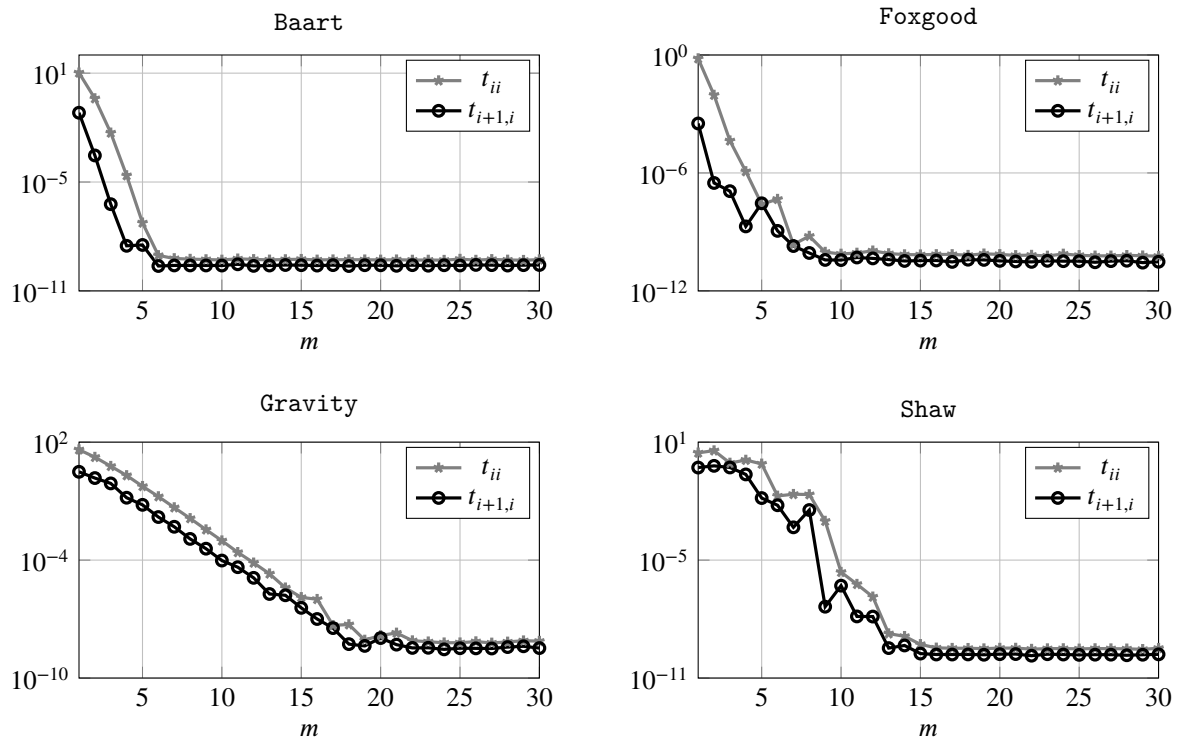

FIGURE 2 Illustration of convergence of the subdiagonal entries $t_{i+1,i}$ and diagonal entries t_{ii} of the tridiagonal matrix T in Theorem 2 to zero. The matrices T are determined by Fredholm integral equations of the first kind described in Section 4.

and, therefore,

$$\mathcal{W}_{m+1} = \mathcal{R}(\mathcal{A}_{h,m+1}) \subset \overline{\mathcal{R}(\mathcal{A}_h \widetilde{P})},$$

which shows (3.16). Furthermore, $\mathcal{R}(\widetilde{Q}_{m+1}\mathcal{A}_{h,m+1}) = \mathcal{R}(\mathcal{A}_{h,m+1})$, which shows (3.17). We have

$$\|\widetilde{Q}_{m+1}(\mathcal{A}_h\widetilde{P} - \mathcal{A}_{h,m})\| \le \|\widetilde{Q}_{m+1}\|\|\mathcal{A}_h\widetilde{P} - \mathcal{A}_{h,m}\| \overset{(3.14)}{\le} \gamma_{m+1}$$

and

$$\|\widetilde{Q}_{m+1}(y - y^\delta)\|_{\mathcal{Y}} \le \|y - y^\delta\|_{\mathcal{Y}} \overset{(1.2)}{\le} \delta.$$

This shows (3.18) and (3.19).

Finally, let $f \in \mathcal{R}(U)$ with $U = [u_1, u_2, \dots\ ]$. The functions u_j form an orthonormal basis for $\mathcal{R}(U)$. We have for coefficients α_j that

$$f = \sum_{j=1}^{\infty} \alpha_j u_j, \quad \sum_{j=1}^{\infty} |\alpha_j|^2 < \infty.$$

The convergence of the latter sum implies that for any arbitrarily small $\eta > 0$, there is an $m = m_\eta$ such that

$$\|f - \widetilde{Q}_{m+1} f\|_{\mathcal{Y}}^2 = \sum_{j=m+2}^{\infty} |\alpha_j|^2 < \eta.$$

This shows (3.20). □

We are in a position to derive a bound for $\|x_{\mu,m+1}^{h,\delta} - x_{\text{exact}}\|_{\mathcal{X}}$.

Lemma 1. Let $x_{\mu,m+1}^{h,\delta}$ be defined by (3.4), let $y \in \mathcal{R}(\mathcal{A})$, and assume that Proposition 1 holds. Then, for any $0 < \mu < \infty$,

$$\|x_{\mu,m+1}^{h,\delta} - x_{\text{exact}}\|_{\mathcal{X}} \le \frac{1}{2\sqrt{\mu}}\left(\delta + \gamma_{m+1}\|x_{\text{exact}}\|_{\mathcal{X}}\right) + h\left(\frac{\|y\|_{\mathcal{Y}}}{\mu} + c + O(h)\right)\|\widetilde{P}_{m+1}\mathcal{A}^*\widetilde{Q}_{m+1}^* y\|_{\mathcal{X}}$$
$$+ \mu\|(\mathcal{A}_{m+1}^*\mathcal{A}_{m+1} + \mu I)^{-1} x_{\text{exact}}\|_{\mathcal{Y}}, \tag{3.21}$$

where c is a constant that is independent of δ, μ, and m, and $\mathcal{A}_{m+1} = \widetilde{Q}_{m+1}\mathcal{A}\widetilde{P}_{m+1}$.

Proof. Split the error into three parts

$$x^{h,\delta}_{\mu,m+1} - x_{\text{exact}} = (x^{h,\delta}_{\mu,m+1} - x^{h}_{\mu,m+1}) + (x^{h}_{\mu,m+1} - x_{\mu,m+1}) + (x_{\mu,m+1} - x_{\text{exact}}),$$

where

$$x^{h}_{\mu,m+1} = \left(\mathcal{A}^*_{h,m+1}\mathcal{A}_{h,m+1} + \mu I\right)^{-1}\mathcal{A}^*_{h,m+1}y,$$
$$x_{\mu,m+1} = \left(\mathcal{A}^*_{m+1}\mathcal{A}_{m+1} + \mu I\right)^{-1}\mathcal{A}^*_{m+1}y$$

and $\mathcal{A}_{h,m+1}$ is defined by (3.4). For any operator $\mathcal{B}$, one can easily show that

$$\|\left(\mathcal{B}^*\mathcal{B} + \mu I\right)^{-1}\mathcal{B}^*\|_{\mathcal{X}} \leq \frac{1}{2\sqrt{\mu}}. \tag{3.22}$$

This inequality and (1.2) yield

$$\|x^{h,\delta}_{\mu,m+1} - x^{h}_{\mu,m+1}\|_{\mathcal{X}} \leq \frac{\delta}{2\sqrt{\mu}}. \tag{3.23}$$

Using the definitions, the second part can be written as

$$\begin{aligned} x^{h}_{\mu,m+1} - x_{\mu,m+1} &= \left(\mathcal{A}^*_{h,m+1}\mathcal{A}_{h,m+1} + \mu I\right)^{-1}\mathcal{A}^*_{h,m+1}y - \left(\mathcal{A}^*_{m+1}\mathcal{A}_{m+1} + \mu I\right)^{-1}\mathcal{A}^*_{m+1}y \\ &= \left(\widetilde{P}_{m+1}\mathcal{A}^*_h\widetilde{Q}_{m+1}\mathcal{A}_h\widetilde{P}_{m+1} + \mu I\right)^{-1}\widetilde{P}_{m+1}\mathcal{A}^*_h\widetilde{Q}_{m+1}y - \left(\widetilde{P}_{m+1}\mathcal{A}^*\widetilde{Q}_{m+1}\mathcal{A}\widetilde{P}_{m+1} + \mu I\right)^{-1}\widetilde{P}_{m+1}\mathcal{A}^*\widetilde{Q}_{m+1}y, \end{aligned}$$

where we have used that $\widetilde{Q}^*_{m+1}\widetilde{Q}_{m+1} = \widetilde{Q}_{m+1}$, $\widetilde{P}^*_{m+1}\widetilde{P}_{m+1} = \widetilde{P}_{m+1}$, $\widetilde{Q}^*_{m+1} = \widetilde{Q}_{m+1}$, and $\widetilde{P}^*_{m+1} = \widetilde{P}_{m+1}$.

Let $M_h = \widetilde{P}_{m+1}\mathcal{A}^*_h\widetilde{Q}_{m+1}\mathcal{A}_h\widetilde{P}_{m+1}$ and $M = \widetilde{P}_{m+1}\mathcal{A}^*\widetilde{Q}_{m+1}\mathcal{A}^*\widetilde{P}_{m+1}$. We have

$$x^{h}_{\mu,m+1} - x_{\mu,m+1} = \left(M_h + \mu I\right)^{-1}\widetilde{P}_{m+1}\left(\mathcal{A}^*_h - \mathcal{A}^*\right)\widetilde{Q}_{m+1}y + \left(\left(M_h + \mu I\right)^{-1} - (M + \mu I)^{-1}\right)\widetilde{P}_{m+1}\mathcal{A}^*\widetilde{Q}_{m+1}y.$$

Since $\|\left(M_h + \mu I\right)^{-1}\| \leq \mu^{-1}$ and $\|\widetilde{P}_{m+1}\left(\mathcal{A}^*_h - \mathcal{A}^*\right)\widetilde{Q}_{m+1}\| \leq h$, it follows that

$$\|x^{h}_{\mu,m+1} - x_{\mu,m+1}\|_{\mathcal{X}} \leq \frac{h\,\|y\|_{\mathcal{Y}}}{\mu} + \|\left(\left(M_h + \mu I\right)^{-1} - (M + \mu I)^{-1}\right)\widetilde{P}_{m+1}\mathcal{A}^*\widetilde{Q}_{m+1}y\|_{\mathcal{X}}.$$

Let $M_h = M + E_h$. Then

$$\begin{aligned} \left(M_h + \mu I\right)^{-1} - (M + \mu I)^{-1} &= (M + \mu I)^{-1}\left(\left(I + (M + \mu I)\,E_h\right)^{-1} - I\right) \\ &= -E_h + O\left(\|E_h\|^2\right). \end{aligned}$$

Using the fact that $\|E_h\| \leq c\,h$ for some constant $c > 0$, we get

$$\|x^{h}_{\mu,m+1} - x_{\mu,m+1}\|_{\mathcal{X}} \leq h\left(\frac{\|y\|_{\mathcal{Y}}}{\mu} + c + O(h)\right)\|\widetilde{P}_{m+1}\mathcal{A}^*\widetilde{Q}_{m+1}y\|_{\mathcal{X}}. \tag{3.24}$$

We turn to the last part:

$$\begin{aligned} x_{\mu,m+1} - x_{\text{exact}} &= \left(\mathcal{A}^*_{m+1}\mathcal{A}_{m+1} + \mu I\right)^{-1}\mathcal{A}^*_{m+1}y - x_{\text{exact}} \\ &= \left(\mathcal{A}^*_{m+1}\mathcal{A}_{m+1} + \mu I\right)^{-1}\mathcal{A}^*_{m+1}\mathcal{A}\,x_{\text{exact}} - x_{\text{exact}}, \qquad (y = \mathcal{A}x_{\text{exact}}) \\ &= \left(\mathcal{A}^*_{m+1}\mathcal{A}_{m+1} + \mu I\right)^{-1}\mathcal{A}^*_{m+1}\left(\mathcal{A}_{m+1} + \left(\mathcal{A} - \mathcal{A}_{m+1}\right)\right)x_{\text{exact}} - x_{\text{exact}}. \end{aligned}$$

By applying (3.14) and (3.22), we obtain

$$\begin{aligned} \|x_{\mu,m+1} - x_{\text{exact}}\|_{\mathcal{X}} &\leq \|\left(\mathcal{A}^*_m\mathcal{A}_{m+1} + \mu I\right)^{-1}\mathcal{A}^*_{m+1}\mathcal{A}_{m+1}x_{\text{exact}} - x_{\text{exact}}\|_{\mathcal{X}} + \frac{\gamma_{m+1}}{2\sqrt{\mu}}\|x_{\text{exact}}\|_{\mathcal{X}} \\ &= \mu\|\left(\mathcal{A}^*_{m+1}\mathcal{A}_{m+1} + \mu I\right)^{-1}x_{\text{exact}}\|_{\mathcal{X}} + \frac{\gamma_{m+1}}{2\sqrt{\mu}}\|x_{\text{exact}}\|_{\mathcal{X}}. \end{aligned} \tag{3.25}$$

Combining (3.23), (3.24), and (3.25) shows the lemma. □

Using the error estimate (3.21), we obtain the following convergence rate results from[21] Proposition 2.6.

Proposition 2. Let $x_{\mu,m+1}^{h,\delta}$ be defined by (3.4) and assume that

$$x_{\text{exact}} = \left(\mathcal{A}_h^*\mathcal{A}_h\right)^{\nu} v_h, \qquad v_h \in \mathcal{N}(\mathcal{A}_h)^{\perp}, \qquad v_h \neq 0, \tag{3.26}$$

for some $\nu \in [0,1]$ with v_h uniformly bounded for all $h > 0$ sufficiently small. Let the regularization parameter

$$\bar{\mu} = \mu\left(\mathcal{W}_{m+1}, \gamma_{m+1}, \mathcal{A}_{h,m+1}, \delta, y^{\delta}\right) > 0$$

satisfy

$$\mu^{3/2}\| \left(\mathcal{A}_{h,m+1}^*\mathcal{A}_{h,m+1} + \mu I\right)^{-1} \left(\mathcal{A}_{h,m+1}^*\mathcal{A}_{h,m+1}\right)^{\nu} v_h\|_{\mathcal{Y}} = \left(\gamma_{m+1}\|x_{\text{exact}}\|_{\mathcal{X}} + \frac{1}{2}\mu\right). \tag{3.27}$$

Then $\mu\left(\mathcal{W}_{m+1}, \gamma_{m+1}, \mathcal{A}_{h,m}, \delta, y^{\delta}\right) \to 0$ as $m \to \infty$ and $\gamma_{m+1}, \delta \to 0$. Moreover,

$$\|x_{\bar{\mu},m+1}^{h,\delta} - x_{\text{exact}}\|_{\mathcal{X}} = o\left(\left(\delta + \gamma_{m+1}\right)^{2\nu/(\nu+1)}\right) + p(m+1,\nu), \tag{3.28}$$

where $o(\cdot)$ has to be replaced by $O(\cdot)$ if $\nu = 1$ and

$$p(m+1,\nu) = \begin{cases} 0, & \text{if } \nu = 0, \\ \xi_{m+1}\|(I - \widetilde{Q}_{m+1})z\|_{\mathcal{Y}}, & \text{if } \nu = \frac{1}{2},\ \ \mathcal{A}_h^*z = \left(\mathcal{A}_h^*\mathcal{A}_h\right)^{1/2} v_h, \\ \xi_{m+1}\|(I - \widetilde{Q}_{m+1})\mathcal{A}_h v_h\|_{\mathcal{Y}} \le \xi_{m+1}^2\|v_h\|_{\mathcal{Y}}, & \text{if } \nu = 1, \\ (4/\pi)\,\xi_{m+1}^{2\nu}\|v_h\|_{\mathcal{Y}}, & \text{otherwise,} \end{cases}$$

and $\xi_{m+1} = \|(I - \widetilde{Q}_{m+1})\mathcal{A}_h\|$.

Remark 2. The standard smoothness condition for obtaining convergence rates in inverse problems, also used by Neubauer[21], reads $x_{\text{exact}} = (\mathcal{A}^*\mathcal{A})v$. In contrast, we require (3.26) to hold for x_{exact} and each h with associated source element v_h and uniform bound $\|v_h\| \le \rho$. This condition has already been used in proving convergence rates for Arnoldi-Tikhonov regularization[23] Proposition 4.2. In real applications, (3.26) might be hard to verify. For a discussion of (3.26), we refer the reader to[23] Remark 4.3 and Proposition 4.5.

The convergence rate in (3.28) is usually optimal with respect to δ and γ_{m+1}. However, the choice of the regularization parameter $\bar{\mu}$ of Proposition 2 is not computable, since v is not known and ν typically is not available. Following Neubauer, we use[21] Theorem 3.5 to obtain an a posteriori parameter selection method, which yields the same rate as in Proposition 2, but only uses available data.

Proposition 3. Let the constants $L > 1$ and $E > 3\|x_{\text{exact}}\|_{\mathcal{X}}$ be such that

$$0 \le E\gamma_{m+1} + L\delta \le \|\widetilde{Q}_{m+1}y^{\delta}\|_{\mathcal{Y}}$$

holds. For x_{exact} let (3.27) be fulfilled, and let $x_{\hat{\mu},m+1}^{h,\delta}$ be defined by (3.4) such that $\hat{\mu}$ is the unique solution of

$$\hat{\mu}^3\left\langle \left(\mathcal{A}_{h,m+1}\mathcal{A}_{h,m+1}^* + \hat{\mu}I\right)^{-3}\widetilde{Q}_{m+1}y^{\delta}, \widetilde{Q}_{m+1}y^{\delta}\right\rangle = \left(E\gamma_m + L\delta\right)^2. \tag{3.29}$$

Then the same asymptotic estimates hold for $x_{\hat{\mu},m+1}^{h,\delta} - x_{\text{exact}}$ as for $x_{\bar{\mu},m+1}^{h,\delta} - x_{\text{exact}}$ in Proposition 2.

The approach for selecting the parameter μ described in Proposition 3 does not tell us how to choose the constants L and E when solving actual problems. We would like these constants to be such that $\|x_{\mu,m+1}^{h,\delta} - x_{\text{exact}}\|_{\mathcal{X}}$ is as small as possible for given values of m, γ_{m+1}, and δ. Results of[21] Proposition 3.6 show that Proposition 3 also holds for $L \ge 1$ and $E \ge \|x_{\text{exact}}\|_{\mathcal{X}}$, and that the best choices of these constants are $L = 1$ and $E = \|x_{\text{exact}}\|_{\mathcal{X}}$.

However, we may not know an accurate estimate of $\|x_{\text{exact}}\|_{\mathcal{X}}$. In this case, Neubauer[21] suggests to let $\bar{\mu} = \mu\left(m+1, \gamma_{m+1}, \delta\right)$ be the unique solution of

$$\bar{\mu}^3\left\langle \left(\mathcal{A}_{h,m+1}\mathcal{A}_{h,m+1}^* + \bar{\mu}I\right)^{-3}\widetilde{Q}_{m+1}y^{\delta}, \widetilde{Q}_{m+1}y^{\delta}\right\rangle = \left(D\gamma_{m+1}\|x_{\mu,m+1}^{h,\delta}\|_{\mathcal{X}} + \delta\right)^2 \tag{3.30}$$

for some constant $D > 1$. Observe that $\|x_{\mu,m+1}^{h,\delta}\|_{\mathcal{X}}$ is a decreasing function of μ and, thus, a solution of (3.30) exists if

$$\delta < \|\widetilde{Q}_{m+1}y^{\delta}\|_{\mathcal{Y}}$$

holds. Let $\hat{\mu}$ be the solution of (3.29) with $L = 1$ and $E = \|x_{\text{exact}}\|_{\mathcal{X}}$, and let $\tilde{\mu}$ be the solution of (3.29) with $L = 1$ and $E = 2D\|x_{\text{exact}}\|_{\mathcal{X}}$. For some constant $D > 1$, we obtain that $\hat{\mu} \leq \bar{\mu} \leq \tilde{\mu}$ and, therefore,

$$\|x^{h,\delta}_{\hat{\mu},m+1} - x_{\text{exact}}\|_{\mathcal{X}} \leq \|x^{h,\delta}_{\bar{\mu},m+1} - x_{\text{exact}}\|_{\mathcal{X}} \leq \|x^{h,\delta}_{\tilde{\mu},m+1} - x_{\text{exact}}\|_{\mathcal{X}}$$

for m sufficiently large, and both h and δ sufficiently small. This provides a computable method for selecting a value of the parameter μ, since we do not need any information about the exact solution x_{exact} or the parameter ν.

In our analysis, we require that the basis of the discretized space does not change when we decrease the noise level. To this end, we fix the noise level and therefore the initial function $\mathcal{A}_h\mathcal{A}_h^* y^\delta$ when applying bidiagonalization. If subsequently the amount of error is decreased, and this requires more bidiagonalization steps to be carried out to satisfy (3.30), then we keep the functions, say $\{u_j\}_{j=1}^{m+1}$ and $\{v_j\}_{j=1}^{m+1}$ already available, and generate more functions u_j and v_j for $j > m+1$ as necessary to satisfy (3.30).

We finally comment on the evaluation of the expression

$$\left\langle \left(\mathcal{A}_{h,m+1}\mathcal{A}_{h,m+1}^* + \hat{\mu} I\right)^{-3} \widetilde{Q}_{m+1} y^\delta, \widetilde{Q}_{m+1} y^\delta \right\rangle$$

in the left-hand side of (3.29). In actual computations, the number of bidiagonalization steps $m+1$ typically is fairly small. It is then convenient to evaluate (3.29) by first computing the singular value decomposition of $\mathcal{A}_{h,m+1}$ by evaluating the singular value decomposition of the lower bidiagonal matrix $C_{m+1,m+1}$ associated with $\mathcal{A}_{h,m+1}$, cf. (3.6), and then using this decomposition to solve

$$(\mathcal{A}_{h,m+1}\mathcal{A}_{h,m+1}^* + \hat{\mu} I)z = \widetilde{Q}_{m+1} y^\delta$$

for z. This is followed by solving another system of equation with the same operator and right-hand side z.

4 | NUMERICAL EXPERIMENTS

In this section, we apply Golub–Kahan bidiagonalization with Tikhonov regularization to solve integral equations of the first kind

$$\int_{\Omega_1} \kappa(s,t)x(t)\,dt = y(s), \qquad s \in \Omega_2, \tag{4.1}$$

where $x \in L^2(\Omega_1)$, $y \in L^2(\Omega_2)$, and $\kappa \in L^2(\Omega_1 \times \Omega_2)$ is a nondegenerate kernel. The Ω_i are subsets of $\mathbb{R}^{d_i}$ for $i = 1, 2$. We first consider four test problems from Regularization Tools [14]; they are problems in one space-dimension and are listed in Table 1. For two test problems, `Gravity` and `Shaw`, the function $y(s)$ is not explicitly known and, therefore, not given explicitly in the table. Instead, it is computed by evaluating the integral (4.1). Subsequently, we apply Golub–Kahan bidiagonalization with Tikhonov regularization to solve an inverse problem in two space-dimensions. This problem is inspired by the IR TOOLS package [11].

All computations were carried out in MATLAB R2017a with about 15 significant decimal digits, some with the MATLAB package Chebfun, running on a laptop computer with core CPU Intel(R) Core(TM)i7-7Y75 @1.60GHz processor with 16GB of RAM. Chebfun carries out computations with approximations of continuous functions and operators. The functions and operators are approximated by piece-wise Chebyshev polynomials, so called chebfuns; see [2, 6] for details. Chebfun makes it unnecessary for a user to explicitly discretize functions and operators. This makes the computations closer to the theory developed in, e.g., Engl et al. [7], than when using the more common approach of discretizing the integral equation (4.1) before solution.

The most common approach to solve the integral equation (4.1) is to first discretize the equation to obtain a linear system of algebraic equations. The matrix of this system will be ill-conditioned. This approach requires that the integrals be approximated by quadrature rules. One can choose the quadrature rules so that the error caused by this approximation is insignificant compared to the regularization error caused by noisy data. We discretize the integral equation (4.1) by a Nyström method based on the composite trapezoidal rule with n nodes. This transforms (4.1) into a linear system of equations $A\boldsymbol{x} = \boldsymbol{y}$, where $A \in \mathbb{R}^{n\times n}$ is a symmetric or nonsymmetric matrix, $\boldsymbol{x} \in \mathbb{R}^n$ is a discretization of the exact solution, x_{exact}, and $\boldsymbol{y} \in \mathbb{R}^n$ is considered an error-free right-hand side vector. We carry out these computations using standard MATLAB (without Chebfun).

We turn to the continuous solution approach that is based on the use of Chebfun. Then $\|\cdot\|_{\Omega_i}$ stands for an L^2-norm. Thus,

$$\|x(t)\|^2_{\Omega_i} = \int_{\Omega_i} |x(t)|^2\,dt, \quad \text{for } i = 1, 2.$$

TABLE 1 Test problems used for the numerical experiments.

Example	Domain	$\kappa(s,t)$, $x(t)$ and $y(s)$	Reference
`Baart`	$\Omega_1 = [0, \pi]$	$\kappa(s,t) = \exp(s\,\cos(t))$	[3] Ex. 4.2
	$\Omega_2 = [0, \frac{\pi}{2}]$	$x(t) = \sin(t)$	
		$y(s) = 2\,\frac{\sinh(s)}{s}$	
`Foxgood`	$\Omega_1 = [0, 1]$	$\kappa(s,t) = (s^2 + t^2)^{\frac{1}{2}}$	[10] p. 520
	$\Omega_2 = [0, 1]$	$x(t) = t$	
		$y(s) = \frac{1}{3}(1 + s^2)^{\frac{3}{2}} - s^3$	
`Gravity`	$\Omega_1 = [0, 1]$	$\kappa(s,t) = (1 + (s-t)^2)^{-\frac{3}{2}}$	[27] p. 17
	$\Omega_2 = [0, 1]$	$x(t) = \sin(t\pi) + \frac{1}{2}\sin(2\pi\, t)$	
`Shaw`	$\Omega_1 = [-\frac{\pi}{2}, \frac{\pi}{2}]$	$\kappa(s,t) = (\cos(s) + \cos(t))\left(\frac{\sin(u)}{u}\right)^2$	[25] p. 97
	$\Omega_2 = [-\frac{\pi}{2}, \frac{\pi}{2}]$	$u = \pi(\sin(s) + \sin(t))$	
		$x(t) = 2e^{-6(t-0.8)^2} + e^{-2(t+0.5)^2}$	

We generate the perturbed operator $\mathcal{A}_h$ associated with the operator $\mathcal{A}$ according to

$$(\mathcal{A}_h x)(s) = \int_{\Omega_1} \kappa^{\alpha}(s,t)\, x(t) dt,$$

where

$$\kappa^{\alpha}(s,t) = \kappa(s,t) + \alpha \frac{\|\kappa(s,t)\|_{\Omega_{1,2}}}{\|F(s,t)\|_{\Omega_{1,2}}} F(s,t).$$

Here, $F(s,t)$ is a smooth Chebfun function in two space-dimensions, generated by the Chebfun command `randnfun2(`ϑ`,`$\Omega_1 \times \Omega_2$`)`, with maximum frequency about $2\pi/\vartheta$ and standard normal distribution $N(0,1)$ at each point. The parameter $\alpha > 0$ specifies the noise level.

The right-hand side function $y(s)$ in (1.1) is assumed not to be known, but the error-contaminated function $y^{\delta}(s)$, defined by

$$y^{\delta}(s) = y(s) + \delta \frac{\|y(s)\|_{\Omega_2}}{\|F(s)\|_{\Omega_2}} F(s),$$

is available. The function $F(s)$ is a smooth Chebfun function, generated with the Chebfun command `randnfun(`ϑ`,`Ω_2`)`, with maximum frequency about $2\pi/\vartheta$ and standard normal distribution $N(0,1)$ at each point. The parameter $\delta > 0$ specifies the noise level. In the computed examples, we let $\vartheta = 10^{-2}$.

Application of $m+1$ steps of the continuous Golub–Kahan bidiagonalization process to the operator $\mathcal{A}_h$ with initial function $u_1 = \mathcal{A}_h \mathcal{A}_h^* y^{\delta} / \|\mathcal{A}_h \mathcal{A}_h^* y^{\delta}\|_{\mathcal{Y}}$ yields the decomposition (2.1), as well as the low-rank operator $\mathcal{A}_{h,m+1}$ as defined by (3.6). Tikhonov regularization is applied to determine an approximate solution of the operator equation

$$\mathcal{A}_{h,m+1} x = y^{\delta}$$

as described in Section 3. In particular, the regularized solution $x_{\mu,m+1}^{h,\delta}$ is computed by using (3.4).

Figures 3 to 6 show some graphs obtained by applying Golub–Kahan bidiagonalization with Tikhonov regularization to the test problems `Baart`, `Foxgood`, `Gravity`, and `Shaw`. The exact kernels $\kappa(s,t)$ and the added errors are illustrated in subfigures (a) and (b), respectively, of all the figures. Subfigures (c) of the figures display the right-hand side functions $y(s)$ and the corresponding error-contaminated functions $y^{\delta}(s)$. The subfigures (d) show the exact solutions $x_{\text{exact}}(t)$ and the computed approximate solutions $x_{\mu,m+1}^{h,\delta}(t)$ determined by applying Golub–Kahan bidiagonalization with Tikhonov regularization for $m = 20$. The latter subfigures show Golub–Kahan bidiagonalization with Tikhonov regularization to yield quite accurate approximations of the exact solution for all the test problems. We let $\alpha = \delta \in \{10^{-4}, 10^{-2}\}$ in all experiments.

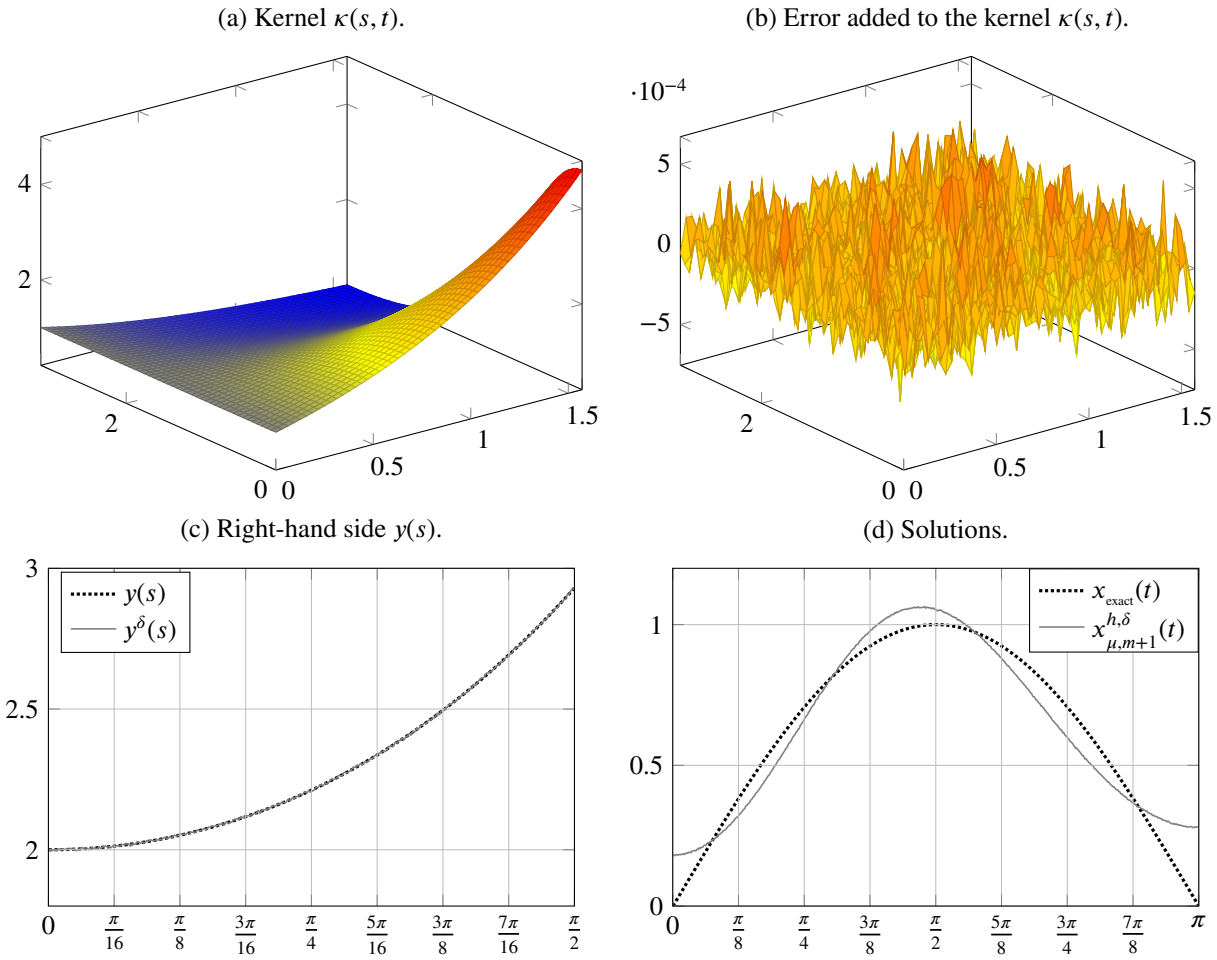

FIGURE 3 Example –"`Baart`", $\alpha = \delta = 1.00\,\text{e}{-4}$.

The second and fourth columns of Table 2 display results for $m \in \{20, 30, 40\}$. The approximation error in the operator $\mathcal{A}$ is evaluated by

$$h = \|(\mathcal{A}x)(s) - (\mathcal{A}_h x)(s)\|_{\Omega_2},$$

which is listed in the third column of Table 2. The fifth column of the table reports the error incurred by replacing the operator $\mathcal{A}_h$ by $\mathcal{A}_{h,m+1}$,

$$\gamma_{m+1} = \|(\mathcal{A}_h x)(s) - (\mathcal{A}_{h,m+1} x)(s)\|_{\Omega_2}.$$

The sixth column displays the value of the regularization parameter μ, which is determined by solving (3.29) with $E = \|x_{\text{exact}}\|_{\Omega_1}$ and $L = 1$ as suggested in the previous section. The desired value of μ is computed by Newton's method with $\delta = \|y - y^{\delta}\|_{\Omega_2}$.

We measure the accuracy of the computed approximate solution $x^{h,\delta}_{\mu,m+1}$ by the relative error

$$RE = \frac{\|x_{\text{exact}} - x^{h,\delta}_{\mu,m+1}\|_{\Omega_1}}{\|x_{\text{exact}}\|_{\Omega_1}}; \tag{4.2}$$

this error is tabulated in the last column of Table 2.

A few observations about Table 2 are in order. The relative error (4.2) depends on the error in the right-hand side function $y^{\delta}(s)$, the error in the approximate operator $\mathcal{A}_h$, and the approximation error γ_{m+1}. We notice that the error γ_{m+1} decreases as the number of bidiagonalization steps m increases, as can be expected from Lemma 2. As a result, when the noise level δ decreases, and the number of bidiagonalization steps m increases, the quality of the computed solutions improves. The results in Table 2 show Golub–Kahan bidiagonalization with Tikhonov regularization using Chebfun to perform well for all test problems considered.

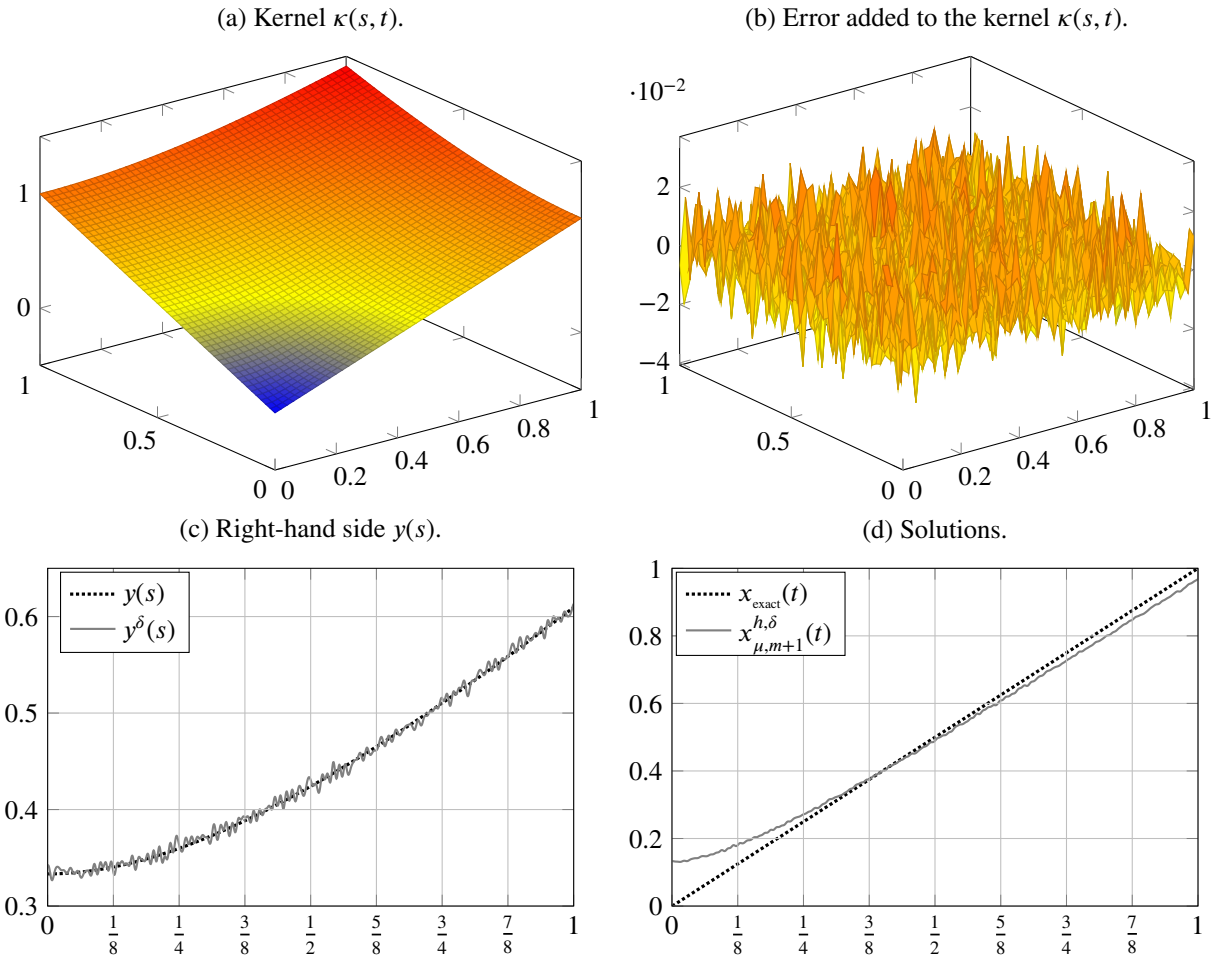

FIGURE 4 Example –"Foxgood", $\alpha = \delta$ =1.00 e−2.

We turn to the discrete approach. Thus, we apply the discrete Golub–Kahan bidiagonalization method with Tikhonov regularization to linear systems of equations

$$A\boldsymbol{x} = \boldsymbol{y}^{\delta}, \qquad A \in \mathbb{R}^{n\times n}, \quad \boldsymbol{x}, \boldsymbol{y}^{\delta} \in \mathbb{R}^{n},$$

that result from the discretization of the operator equation (4.1). In this approach, $\|\cdot\|_2$ denotes the Euclidean vector norm or the associated induced matrix norm. We define the perturbed matrix $A_h \in \mathbb{R}^{n\times n}$ by

$$A_h = A + \alpha \frac{\|A\|_2}{\|\tilde{F}\|_2}\tilde{F},$$

where $\tilde{F} \in \mathbb{R}^{n\times n}$ is a random matrix whose entries are from a normal distribution with mean zero and variance one, and α is a chosen error level. We generate the error-contaminated vector $\boldsymbol{y}^{\delta} \in \mathbb{R}^{n}$ according to

$$\boldsymbol{y}^{\delta} = \boldsymbol{y} + \delta \frac{\|\boldsymbol{y}\|_2}{\|\boldsymbol{e}\|_2}\boldsymbol{e},$$

where $\boldsymbol{e} \in \mathbb{R}^{n}$ is a random vector whose entries are from a normal distribution with mean zero and variance one. Application of a discrete analogue of Algorithm 1 to the matrix A_h with initial vector $\boldsymbol{u}_1 = AA^*\boldsymbol{y}^{\delta}/\|AA^*\boldsymbol{y}^{\delta}\|_2$ yields the decompositions

$$A_h\tilde{V}_m = \tilde{U}_{m+1}\tilde{C}_{m+1,m}, \qquad A_h^*\tilde{U}_m = \tilde{V}_m\tilde{C}^*_{m,m},$$

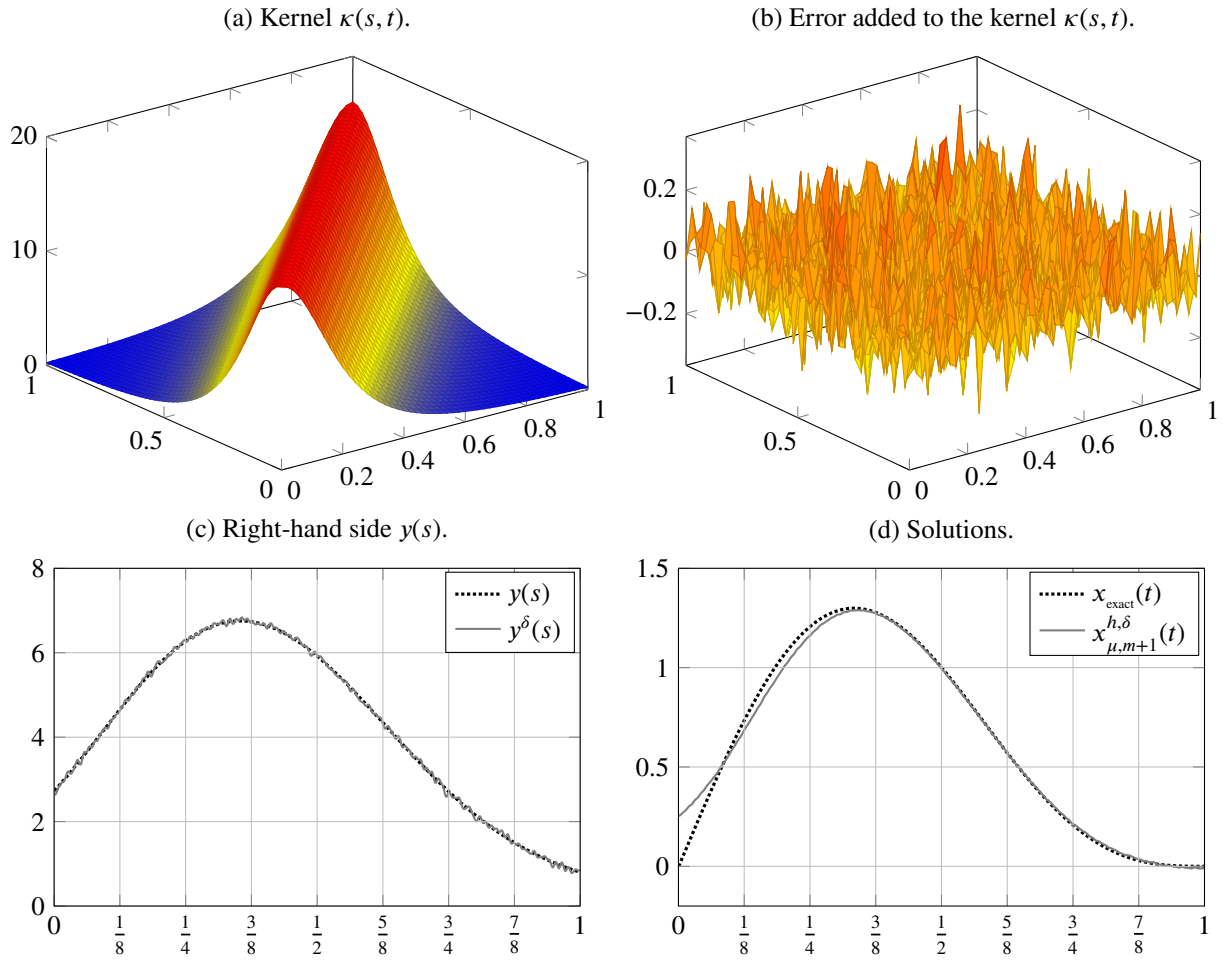

FIGURE 5 Example –"`Gravity`", $\alpha = \delta$ =1.00 e−2.

where the matrices $\tilde{V}_m = [\boldsymbol{v}_1, \boldsymbol{v}_2, \ldots, \boldsymbol{v}_m] \in \mathbb{R}^{n\times m}$ and $\tilde{U}_{m+1} = [\boldsymbol{u}_1, \boldsymbol{u}_2, \ldots, \boldsymbol{u}_{m+1}] \in \mathbb{R}^{n\times(m+1)}$ have orthonormal columns. Moreover,

$$\tilde{C}_{m+1,m} = \begin{bmatrix} \alpha_1 & & & \\ \beta_2 & \alpha_2 & & \\ & \ddots & \ddots & \\ & & \beta_m & \alpha_m \\ & & & \beta_{m+1} \end{bmatrix} \in \mathbb{R}^{(m+1)\times m} \tag{4.3}$$

is a lower bidiagonal matrix. The algorithm also determines the lower bidiagonal matrix $\tilde{C}_{m+1,m+1} \in \mathbb{R}^{(m+1)\times(m+1)}$ with leading principal submatrix (4.3) and the matrix $\tilde{V}_{m+1} = [\boldsymbol{v}_1, \boldsymbol{v}_2, \ldots, \boldsymbol{v}_{m+1}] \in \mathbb{R}^{n\times(m+1)}$. Define the low-rank approximation $A_{h,m+1}$ of the matrix A_h by

$$A_{h,m+1} = \tilde{U}_{m+1}\tilde{C}_{m+1,m+1}\tilde{V}^*_{m+1}.$$

We compute an approximate solution of the linear system of equations

$$A_{h,m+1}\boldsymbol{x} = \boldsymbol{y}^\delta$$

with the aid of Tikhonov regularization. The computed regularized solution $\boldsymbol{x}^{h,\delta}_{\mu,m+1}$ is given by

$$\boldsymbol{x}^{h,\delta}_{\mu,m+1} = \left(A^*_{h,m+1}A_{h,m+1} + \mu I\right)^{-1} A^*_{h,m+1}\boldsymbol{y}^\delta.$$

Tables 3 to 6 report results obtained when applying m steps of discrete Golub–Kahan bidiagonalization with Tikhonov regularization to the `Baart`, `Foxgood`, `Gravity`, and `Shaw` test problems, respectively. In our experiments, we let $\alpha = \delta \in \{10^{-4}, 10^{-2}\}$,

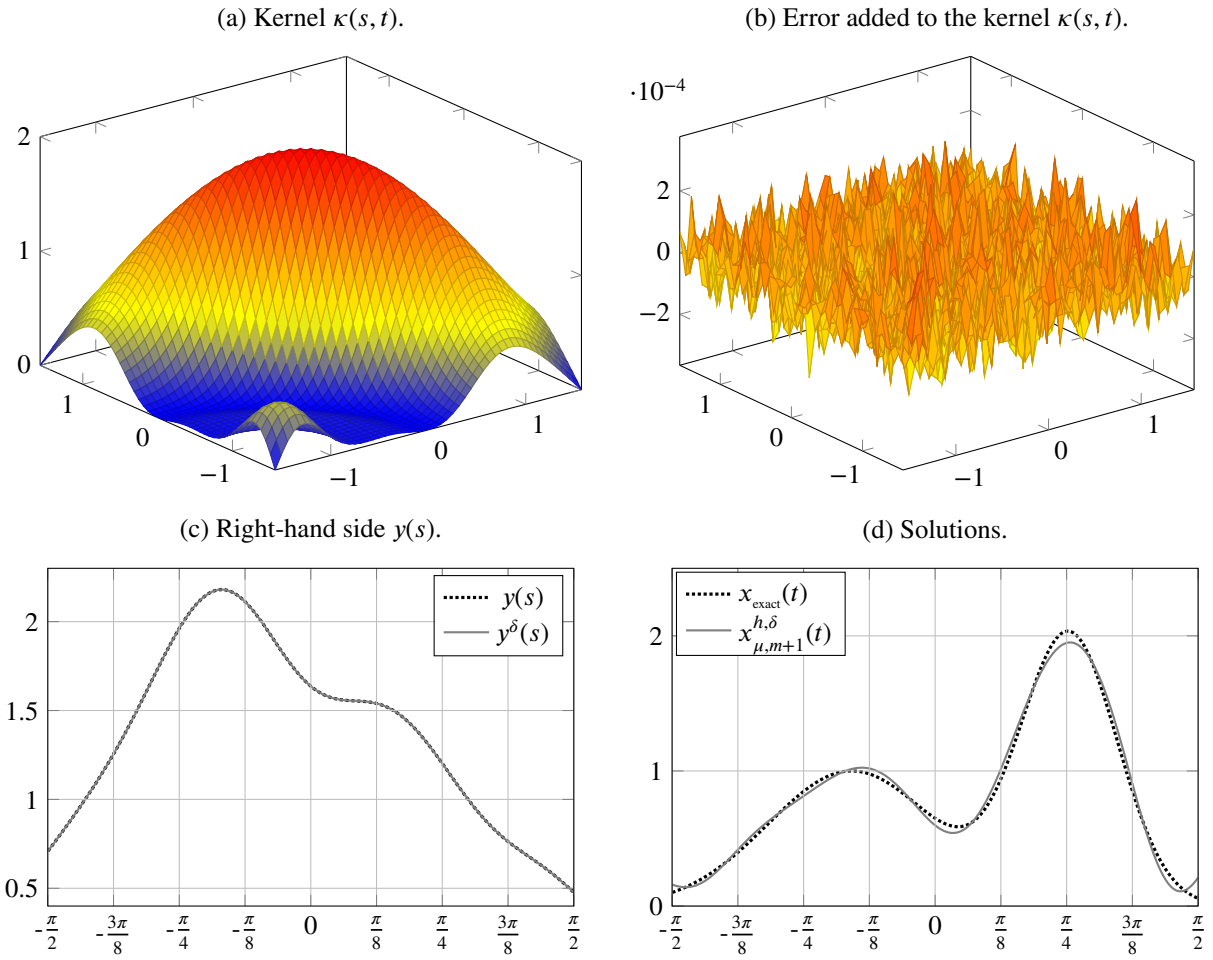

FIGURE 6 Example –"`Shaw`", $\alpha = \delta$ =1.00 e−4.

$n \in \{1000, 2000, 4000\}$, and $m \in \{20, 30, 40\}$, which are listed in the first, second, and fourth columns of the tables, respectively. The approximation error of the matrix A_h is evaluated by

$$h = \|A - A_h\|_2.$$

These errors are displayed in the third column of the tables. The fifth column shows the approximation error that is incurred by approximating the matrix A_h by the low-rank matrix $A_{h,m+1}$; it is computed by

$$\gamma_{m+1} = \|A_h - A_{h,m+1}\|_2.$$

The accuracy of the computed approximation $\boldsymbol{x}^{h,\delta}_{\mu,m+1}$ of $\boldsymbol{x}_{\text{exact}}$ is measured by the relative error

$$RE = \frac{\|\boldsymbol{x}_{\text{exact}} - \boldsymbol{x}^{h,\delta}_{\mu,m+1}\|_2}{\|\boldsymbol{x}_{\text{exact}}\|_2}, \tag{4.4}$$

and is shown in the last column of the tables.

We make the following observations about the results in Tables 3 to 6. The relative error (4.4) in the computed solution depends on the error in the right-hand side function $y^{\delta}(s)$, the error in the operator A_h, and on the approximation error γ_{m+1}. We notice that the relative error decreases as the number of bidiagonalization steps m is increased for fixed n.

Tables 2 to 6 show the computed approximate solutions determined by the continuous GKB-Tikhonov method with Chebfun to give more accurate approximations of the exact solutions x_{exact} than the approximate solutions determined by the discrete GKB-Tikhonov method.

TABLE 2 Results obtained by applying the GKB-Tikhonov method with Chebfun to the `Baart`, `Foxgood`, `Gravity`, and `Shaw` test problems.

Example	Noise level	h	m	γ_{m+1}	μ	RE
`Baart`	10^{-4}	$1.8691 \cdot 10^{-5}$	20	$9.1879 \cdot 10^{-7}$	$2.3465 \cdot 10^{-6}$	$1.1331 \cdot 10^{-1}$
			30	$8.9538 \cdot 10^{-7}$	$2.1411 \cdot 10^{-6}$	$1.1308 \cdot 10^{-1}$
			40	$8.5346 \cdot 10^{-7}$	$2.0492 \cdot 10^{-6}$	$1.1296 \cdot 10^{-1}$
	10^{-2}	$1.8447 \cdot 10^{-3}$	20	$1.9810 \cdot 10^{-4}$	$2.3562 \cdot 10^{-3}$	$1.9569 \cdot 10^{-1}$
			30	$1.8898 \cdot 10^{-4}$	$2.2540 \cdot 10^{-3}$	$1.9423 \cdot 10^{-1}$
			40	$1.8170 \cdot 10^{-4}$	$2.2034 \cdot 10^{-3}$	$1.9350 \cdot 10^{-1}$
`Foxgood`	10^{-4}	$3.5548 \cdot 10^{-6}$	20	$5.7627 \cdot 10^{-10}$	$1.7781 \cdot 10^{-5}$	$1.0782 \cdot 10^{-2}$
			30	$5.3919 \cdot 10^{-10}$	$1.5371 \cdot 10^{-5}$	$1.0110 \cdot 10^{-2}$
			40	$5.0299 \cdot 10^{-10}$	$1.3521 \cdot 10^{-5}$	$9.5829 \cdot 10^{-3}$
	10^{-2}	$3.8030 \cdot 10^{-4}$	20	$1.7885 \cdot 10^{-6}$	$1.8357 \cdot 10^{-3}$	$5.9800 \cdot 10^{-2}$
			30	$1.7111 \cdot 10^{-6}$	$1.4946 \cdot 10^{-3}$	$5.3485 \cdot 10^{-2}$
			40	$1.5477 \cdot 10^{-6}$	$1.2965 \cdot 10^{-3}$	$4.9877 \cdot 10^{-2}$
`Gravity`	10^{-4}	$4.9568 \cdot 10^{-5}$	20	$2.8666 \cdot 10^{-8}$	$2.1567 \cdot 10^{-3}$	$1.3043 \cdot 10^{-2}$
			30	$2.6213 \cdot 10^{-8}$	$1.2988 \cdot 10^{-3}$	$1.1397 \cdot 10^{-2}$
			40	$2.4565 \cdot 10^{-8}$	$1.1183 \cdot 10^{-3}$	$1.0966 \cdot 10^{-2}$
	10^{-2}	$5.6748 \cdot 10^{-3}$	20	$2.9287 \cdot 10^{-5}$	$2.7345 \cdot 10^{-1}$	$5.8208 \cdot 10^{-2}$
			30	$2.7037 \cdot 10^{-5}$	$1.9778 \cdot 10^{-1}$	$5.2284 \cdot 10^{-2}$
			40	$2.5929 \cdot 10^{-5}$	$1.4755 \cdot 10^{-1}$	$4.7811 \cdot 10^{-2}$
`Shaw`	10^{-4}	$2.4056 \cdot 10^{-5}$	20	$1.8517 \cdot 10^{-7}$	$3.8155 \cdot 10^{-5}$	$4.6667 \cdot 10^{-2}$
			30	$1.7918 \cdot 10^{-7}$	$2.1163 \cdot 10^{-5}$	$4.5770 \cdot 10^{-2}$
			40	$1.7575 \cdot 10^{-7}$	$9.0756 \cdot 10^{-6}$	$4.4066 \cdot 10^{-2}$
	10^{-2}	$2.5578 \cdot 10^{-3}$	20	$1.2229 \cdot 10^{-4}$	$6.4269 \cdot 10^{-3}$	$1.1138 \cdot 10^{-1}$
			30	$1.1798 \cdot 10^{-4}$	$5.1209 \cdot 10^{-3}$	$1.0453 \cdot 10^{-1}$
			40	$1.1348 \cdot 10^{-4}$	$4.3765 \cdot 10^{-3}$	$1.0052 \cdot 10^{-1}$

Our last example is concerned with solving an inverse linear PDE problem. We select the inverse `diffusion` problem from the IR TOOLS package[11]. The partial differential equation

$$\dot{u} = u_{t_1,t_1} + u_{t_2,t_2}, \qquad \text{for all } (t_1, t_2) \in \Omega_1 = [0,1] \times [0,1],$$

describes a diffusion process, where $u(t_1, t_2, \tau)$ is the concentration at the point (t_1, t_2) in Ω_1 at time τ. The time derivative of u is denoted by $\dot{u}$, and u_{t_i,t_i} stands for the second derivative in direction t_i. We assume that u satisfies the initial condition

$$u(t_1, t_2, 0) = u_0(t_1, t_2),$$

for some given function u_0, and Neumann boundary conditions for all time $\tau \geq 0$,

$$u_{t_1}(t_1, t_2, \tau) = 0, \qquad \text{for all } (t_1, t_2) \in \partial\Omega_1,$$

where $\partial\Omega_1$ denotes the boundary of Ω_1. After T seconds, the solution of the system is

$$u_T(t_1, t_2) = u(t_1, t_2, T).$$

Our task is to recover the initial condition u_0 from a given noisy version of u_T for $T = 0.01$. To generate data for this problem, we use the MATLAB function

```
[A, y, x, ProbInfo] = PRdiffusion(n)
```

TABLE 3 Results obtained by applying the discrete GKB-Tikhonov method to the `Baart` test problem.

Noise level	n	h	m	γ_{m+1}	μ	RE
10^{-4}	1000	$4.5674 \cdot 10^{-4}$	20	$4.5322 \cdot 10^{-4}$	$3.0481 \cdot 10^{-4}$	$1.5531 \cdot 10^{-1}$
			30	$4.4930 \cdot 10^{-4}$	$2.9385 \cdot 10^{-4}$	$1.5495 \cdot 10^{-1}$
			40	$4.4895 \cdot 10^{-4}$	$2.9285 \cdot 10^{-4}$	$1.5492 \cdot 10^{-1}$
	2000	$4.5667 \cdot 10^{-4}$	20	$4.5342 \cdot 10^{-4}$	$3.2164 \cdot 10^{-4}$	$1.5607 \cdot 10^{-1}$
			30	$4.5297 \cdot 10^{-4}$	$3.2030 \cdot 10^{-4}$	$1.5603 \cdot 10^{-1}$
			40	$4.5120 \cdot 10^{-4}$	$3.1571 \cdot 10^{-4}$	$1.5589 \cdot 10^{-1}$
	4000	$4.5664 \cdot 10^{-4}$	20	$4.5584 \cdot 10^{-4}$	$3.1806 \cdot 10^{-4}$	$1.5588 \cdot 10^{-1}$
			30	$4.5571 \cdot 10^{-4}$	$3.1748 \cdot 10^{-4}$	$1.5586 \cdot 10^{-1}$
			40	$4.5454 \cdot 10^{-4}$	$3.1413 \cdot 10^{-4}$	$1.5576 \cdot 10^{-1}$
10^{-2}	1000	$4.5674 \cdot 10^{-2}$	20	$4.5196 \cdot 10^{-2}$	$2.4122 \cdot 10^{-1}$	$3.6483 \cdot 10^{-1}$
			30	$4.4930 \cdot 10^{-2}$	$2.3934 \cdot 10^{-1}$	$3.6442 \cdot 10^{-1}$
			40	$4.4685 \cdot 10^{-2}$	$2.3795 \cdot 10^{-1}$	$3.6411 \cdot 10^{-1}$
	2000	$4.5667 \cdot 10^{-2}$	20	$4.5355 \cdot 10^{-2}$	$2.3986 \cdot 10^{-1}$	$3.6337 \cdot 10^{-1}$
			30	$4.5278 \cdot 10^{-2}$	$2.3891 \cdot 10^{-1}$	$3.6317 \cdot 10^{-1}$
			40	$4.5134 \cdot 10^{-2}$	$2.3801 \cdot 10^{-1}$	$3.6297 \cdot 10^{-1}$
	4000	$4.5664 \cdot 10^{-2}$	20	$4.5589 \cdot 10^{-2}$	$2.4358 \cdot 10^{-1}$	$3.6510 \cdot 10^{-1}$
			30	$4.5536 \cdot 10^{-2}$	$2.4252 \cdot 10^{-1}$	$3.6487 \cdot 10^{-1}$
			40	$4.5397 \cdot 10^{-2}$	$2.4158 \cdot 10^{-1}$	$3.6466 \cdot 10^{-1}$

TABLE 4 Results obtained by applying the discrete GKB-Tikhonov method to the `Foxgood` test problem.

Noise level	n	h	m	γ_{m+1}	μ	RE
10^{-4}	1000	$8.1109 \cdot 10^{-5}$	20	$8.0417 \cdot 10^{-5}$	$1.2294 \cdot 10^{-4}$	$3.5932 \cdot 10^{-2}$
			30	$7.9794 \cdot 10^{-5}$	$1.2046 \cdot 10^{-4}$	$3.5852 \cdot 10^{-2}$
			40	$7.9706 \cdot 10^{-5}$	$1.1998 \cdot 10^{-4}$	$3.5836 \cdot 10^{-2}$
	2000	$8.1097 \cdot 10^{-5}$	20	$8.0532 \cdot 10^{-5}$	$1.2350 \cdot 10^{-4}$	$3.0527 \cdot 10^{-2}$
			30	$8.0480 \cdot 10^{-5}$	$1.2290 \cdot 10^{-4}$	$3.0504 \cdot 10^{-2}$
			40	$8.0359 \cdot 10^{-5}$	$1.2261 \cdot 10^{-4}$	$3.0493 \cdot 10^{-2}$
	4000	$8.1091 \cdot 10^{-5}$	20	$8.0936 \cdot 10^{-5}$	$1.2405 \cdot 10^{-4}$	$2.7372 \cdot 10^{-2}$
			30	$8.0885 \cdot 10^{-5}$	$1.2352 \cdot 10^{-4}$	$2.7349 \cdot 10^{-2}$
			40	$8.0612 \cdot 10^{-5}$	$1.2291 \cdot 10^{-4}$	$2.7323 \cdot 10^{-2}$
10^{-2}	1000	$8.1109 \cdot 10^{-3}$	20	$8.0400 \cdot 10^{-3}$	$1.3862 \cdot 10^{-2}$	$1.8441 \cdot 10^{-1}$
			30	$8.0396 \cdot 10^{-3}$	$1.3776 \cdot 10^{-2}$	$1.8397 \cdot 10^{-1}$
			40	$8.0068 \cdot 10^{-3}$	$1.3674 \cdot 10^{-2}$	$1.8346 \cdot 10^{-1}$
	2000	$8.1097 \cdot 10^{-3}$	20	$8.0567 \cdot 10^{-3}$	$1.3537 \cdot 10^{-2}$	$1.7979 \cdot 10^{-1}$
			30	$8.0510 \cdot 10^{-3}$	$1.3459 \cdot 10^{-2}$	$1.7937 \cdot 10^{-1}$
			40	$8.0130 \cdot 10^{-3}$	$1.3355 \cdot 10^{-2}$	$1.7882 \cdot 10^{-1}$
	4000	$8.1091 \cdot 10^{-3}$	20	$8.0955 \cdot 10^{-3}$	$1.4008 \cdot 10^{-2}$	$1.8266 \cdot 10^{-1}$
			30	$8.0848 \cdot 10^{-3}$	$1.3897 \cdot 10^{-2}$	$1.8209 \cdot 10^{-1}$
			40	$8.0599 \cdot 10^{-3}$	$1.3807 \cdot 10^{-2}$	$1.8164 \cdot 10^{-1}$

TABLE 5 Results obtained by applying the discrete GKB-Tikhonov method to the `Gravity` test problem.

Noise level	n	h	m	γ_{m+1}	μ	RE
10^{-4}	1000	$6.4596 \cdot 10^{-4}$	20	$6.3987 \cdot 10^{-4}$	$1.0176 \cdot 10^{-2}$	$1.9575 \cdot 10^{-2}$
			30	$6.3314 \cdot 10^{-4}$	$9.8998 \cdot 10^{-3}$	$1.9420 \cdot 10^{-2}$
			40	$6.2825 \cdot 10^{-4}$	$9.8053 \cdot 10^{-3}$	$1.9367 \cdot 10^{-2}$
	2000	$6.4594 \cdot 10^{-4}$	20	$6.4155 \cdot 10^{-4}$	$1.0223 \cdot 10^{-2}$	$1.9787 \cdot 10^{-2}$
			30	$6.3831 \cdot 10^{-4}$	$9.9587 \cdot 10^{-3}$	$1.9640 \cdot 10^{-2}$
			40	$6.3766 \cdot 10^{-4}$	$9.9348 \cdot 10^{-3}$	$1.9627 \cdot 10^{-2}$
	4000	$6.4593 \cdot 10^{-4}$	20	$7.0373 \cdot 10^{-4}$	$1.1048 \cdot 10^{-2}$	$2.0246 \cdot 10^{-2}$
			30	$6.4430 \cdot 10^{-4}$	$1.0062 \cdot 10^{-2}$	$1.9716 \cdot 10^{-2}$
			40	$6.4294 \cdot 10^{-4}$	$1.0037 \cdot 10^{-2}$	$1.9702 \cdot 10^{-2}$
10^{-2}	1000	$6.4596 \cdot 10^{-2}$	20	$6.3992 \cdot 10^{-2}$	$1.6496 \cdot 10^{0}$	$1.1784 \cdot 10^{-1}$
			30	$6.3290 \cdot 10^{-2}$	$1.6271 \cdot 10^{0}$	$1.1707 \cdot 10^{-1}$
			40	$6.3064 \cdot 10^{-2}$	$1.6186 \cdot 10^{0}$	$1.1678 \cdot 10^{-1}$
	2000	$6.4594 \cdot 10^{-2}$	20	$6.4444 \cdot 10^{-2}$	$1.6543 \cdot 10^{0}$	$1.1831 \cdot 10^{-1}$
			30	$6.4212 \cdot 10^{-2}$	$1.6390 \cdot 10^{0}$	$1.1779 \cdot 10^{-1}$
			40	$6.4000 \cdot 10^{-2}$	$1.6305 \cdot 10^{0}$	$1.1750 \cdot 10^{-1}$
	4000	$6.4593 \cdot 10^{-2}$	20	$6.4492 \cdot 10^{-2}$	$1.6574 \cdot 10^{0}$	$1.1870 \cdot 10^{-1}$
			30	$6.4152 \cdot 10^{-2}$	$1.6391 \cdot 10^{0}$	$1.1808 \cdot 10^{-1}$
			40	$6.4096 \cdot 10^{-2}$	$1.6332 \cdot 10^{0}$	$1.1788 \cdot 10^{-1}$

TABLE 6 Results obtained by applying the discrete GKB-Tikhonov method to the `Shaw` test problem.

Noise level	n	h	m	γ_{m+1}	μ	RE
10^{-4}	1000	$2.9988 \cdot 10^{-4}$	20	$1.2597 \cdot 10^{-2}$	$4.7310 \cdot 10^{-2}$	$1.7496 \cdot 10^{-1}$
			30	$1.2596 \cdot 10^{-2}$	$4.7306 \cdot 10^{-2}$	$1.7496 \cdot 10^{-1}$
			40	$1.2595 \cdot 10^{-2}$	$4.7301 \cdot 10^{-2}$	$1.7496 \cdot 10^{-1}$
	2000	$2.9960 \cdot 10^{-4}$	20	$6.3179 \cdot 10^{-3}$	$1.9000 \cdot 10^{-2}$	$1.6057 \cdot 10^{-1}$
			30	$6.3179 \cdot 10^{-3}$	$1.8996 \cdot 10^{-2}$	$1.6057 \cdot 10^{-1}$
			40	$6.3179 \cdot 10^{-3}$	$1.8993 \cdot 10^{-2}$	$1.6057 \cdot 10^{-1}$
	4000	$2.9947 \cdot 10^{-4}$	20	$3.1883 \cdot 10^{-3}$	$3.5123 \cdot 10^{-3}$	$1.2861 \cdot 10^{-1}$
			30	$3.1881 \cdot 10^{-3}$	$3.5085 \cdot 10^{-3}$	$1.2858 \cdot 10^{-1}$
			40	$3.1874 \cdot 10^{-3}$	$3.5054 \cdot 10^{-3}$	$1.2856 \cdot 10^{-1}$
10^{-2}	1000	$2.9988 \cdot 10^{-2}$	20	$3.1927 \cdot 10^{-2}$	$1.8204 \cdot 10^{-1}$	$2.2556 \cdot 10^{-1}$
			30	$3.1747 \cdot 10^{-2}$	$1.8034 \cdot 10^{-1}$	$2.2502 \cdot 10^{-1}$
			40	$3.1535 \cdot 10^{-2}$	$1.7892 \cdot 10^{-1}$	$2.2456 \cdot 10^{-1}$
	2000	$2.9960 \cdot 10^{-2}$	20	$3.0428 \cdot 10^{-2}$	$1.7314 \cdot 10^{-1}$	$2.2136 \cdot 10^{-1}$
			30	$3.0360 \cdot 10^{-2}$	$1.7223 \cdot 10^{-1}$	$2.2106 \cdot 10^{-1}$
			40	$3.0324 \cdot 10^{-2}$	$1.7179 \cdot 10^{-1}$	$2.2091 \cdot 10^{-1}$
	4000	$2.9947 \cdot 10^{-2}$	20	$3.0019 \cdot 10^{-2}$	$1.7299 \cdot 10^{-1}$	$2.2168 \cdot 10^{-1}$
			30	$3.0013 \cdot 10^{-2}$	$1.7224 \cdot 10^{-1}$	$2.2144 \cdot 10^{-1}$
			40	$3.0001 \cdot 10^{-2}$	$1.7190 \cdot 10^{-1}$	$2.2133 \cdot 10^{-1}$

from IR TOOLS, where A is a function handle for the forward and adjoint problem, $y \in \mathbb{R}^N$ is a vector that represents the solution u_T, and $x \in \mathbb{R}^N$ is a vector that represents the initial condition u_0. In this example, we let $N = n^2 = 4096$ and the noise level to be 10^{-4}.

The true solution x_{exact} corresponding to the initial condition to u_0 and the noisy data y^δ corresponding to the function u_T are displayed in subfigures (a) and (b), respectively, of Figure 7. Subfigures (c) and (d) of Figure 7 display values of the regularization parameter μ, the error γ_{m+1}, and the relative error as a function of the number of the iterations $m + 1$ for $m \in \{30, 40, 50, 60\}$. The remaining subfigures illustrate the reconstructed solutions obtained by applying the GKB-Tikhonov method with different values of m. In our experience, $m = 50$ or $m = 60$ seems to produce better results.

5 | CONCLUSION

This paper describes an application of a continuous version of Golub–Kahan bidiagonalization to integral operators of the first kind to determine a low-rank approximation. The effect of this approximation error, as well as of errors in the available integral operator and right-hand side functions on the approximate solution determined by Tikhonov regularization is investigated. Our analysis applies results by Neubauer[21]. Computed results illustrate the theory. The computations are carried out both in the standard way of first discretizing and then solving the discretized problem, and by applying Chebfun which works with functions. The computations with Chebfun are closer to the theory for ill-posed problems described in, e.g.,[7], than the discretize first approach.

ACKNOWLEDGMENT

We would like to thank Andreas Neubauer for comments. The work of RR has been supported by the SFB "Tomography across the Scales", Subproject F6805-N36 funded by the Austrian Science Fund (FWF). Research by LR was supported in part by NSF grant DMS-1720259.

References

1. A. ALQAHTANI, S. GAZZOLA, L. REICHEL, AND G. RODRIGUEZ, *On the block Lanczos and block Golub–Kahan reduction methods applied to discrete ill-posed problems*, Numer. Linear Algebra Appl., 28 (2021), Art. e2376.

2. A. ALQAHTANI, T. MACH, AND L. REICHEL, *Solution of ill-posed problems with Chebfun*, Numer. Algorithms (2022). https://doi.org/10.1007/s11075-022-01390-z

3. M. L. BAART, *The use of auto-correlation for pseudo-rank determination in noisy ill-conditioned linear least-squares problems*, IMA J. Numer. Anal., 2 (1982), pp. 241–247.

4. I. R. BLEYER AND R. RAMLAU, *A double regularization approach for inverse problems with noisy data and inexact operator*, Inverse Problems, 29 (2013), Art. 025004.

5. D. CALVETTI AND L. REICHEL, *Tikhonov regularization of large linear problems*, BIT Numer. Math., 43 (2003), pp. 263–283.

6. T. A. DRISCOLL, N. HALE, AND L. N. TREFETHEN, eds., *Chebfun Guide*, Oxford, 2014.

7. H. W. ENGL, M. HANKE, AND A. NEUBAUER, *Regularization of Inverse Problems*, Kluwer, Dordrecht, 1996.

8. C. FENU, L. REICHEL, AND G. RODRIGUEZ, *GCV for Tikhonov regularization via global Golub–Kahan decomposition*, Numer. Linear Algebra Appl., 23 (2016), pp. 467–484.

9. C. FENU, L. REICHEL, G. RODRIGUEZ, AND H. SADOK, *GCV for Tikhonov regularization by partial SVD*, BIT Numer. Math., 57 (2017), pp. 1019–1039.

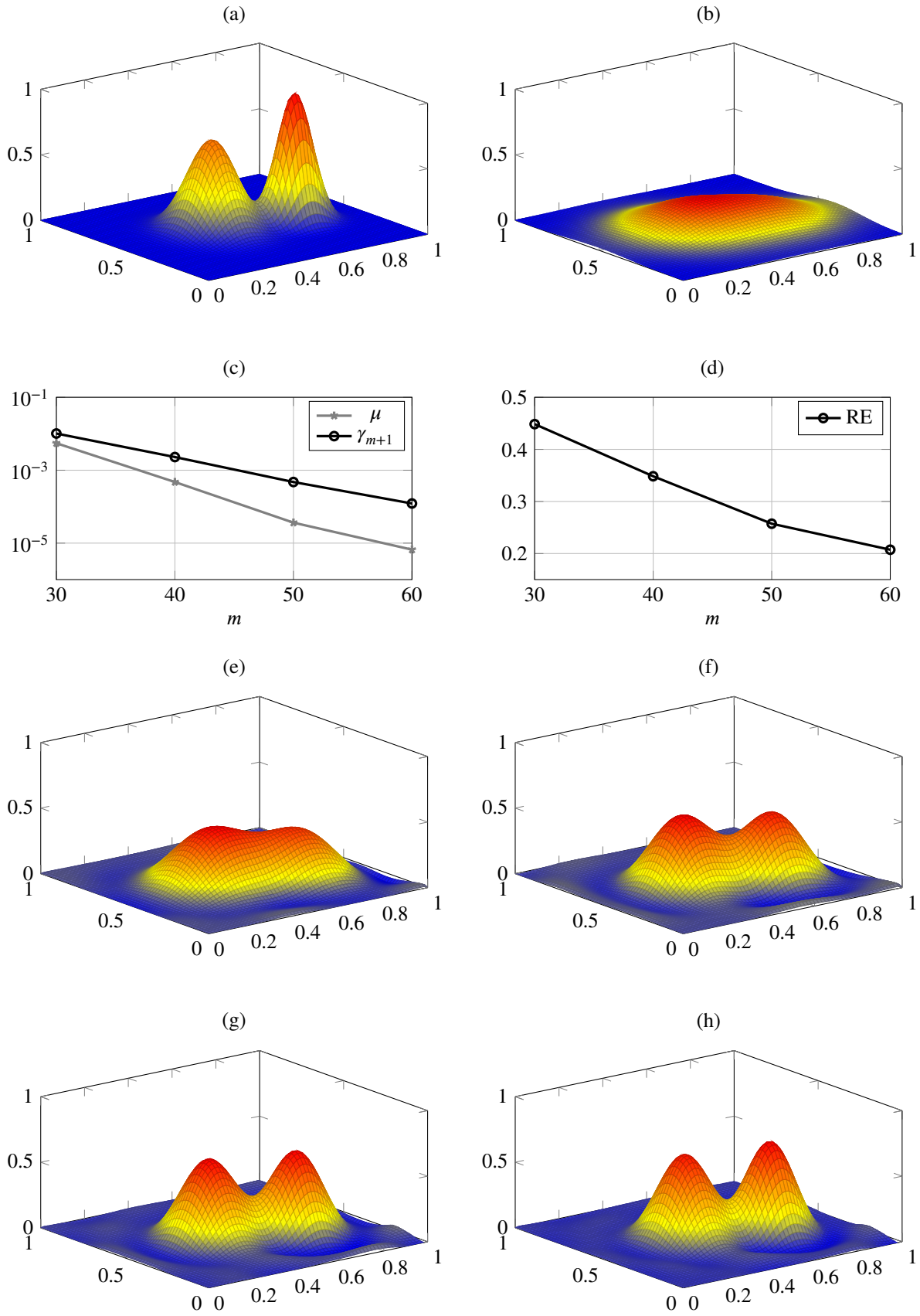

FIGURE 7 Illustration of the solution of the 2D inverse diffusion problem–"PRdiffusion", with n = 64 and $\alpha = \delta = 1.00\,\mathrm{e}{-4}$ by Golub–Kahan bidiagonalization with Tikhonov regularization. (a) true solution x; (b) noisy data $\boldsymbol{y}^{\delta}$; (c) regularization parameter μ and the error γ_{m+1}; (d) the relative error RE; (e–h) reconstruction solutions with $m = 30$, 40, 50 and 60 respectively.

10. L. FOX AND E. T. GOODWIN, *The numerical solution of non-singular linear integral equations*, Philos. Trans. R. Soc. Lond. Ser. A Math. Phys. Eng. Sci., 245:902 (1953) pp. 501–534.

11. S. GAZZOLA, P. C. HANSEN, AND J. G. NAGY, *IR Tools: A MATLAB package of iterative regularization methods and large-scale test problems*, Numer. Algorithms, 81 (2019), pp. 773–811.

12. S. GAZZOLA, P. NOVATI, AND M. R. RUSSO, *On Krylov projection methods and Tikhonov regularization*, Electron. Trans. Numer. Anal., 44 (2015), pp. 83–123.

13. S. GAZZOLA AND M. SABATÈ LANDMAN, *Krylov methods for inverse problems: Surveying classical, and introducing new, algorithmic approaches*, GAMM Mitt., 43 (2020), Art. e202000017.

14. P. C. HANSEN, *Regularization tools version 4.0 for MATLAB 7.3*, Numer. Algorithms, 46 (2007) pp. 189–194.

15. S. KARIMI AND M. JOZI, *A new iterative method for solving linear Fredholm integral equations using the least squares method*, Appl. Math. Comput., 250 (2015), pp. 744–758.

16. S. KINDERMANN, *Convergence analysis of minimization-based noise level-free parameter choice rules for linear ill-posed problems*, Electron. Trans. Numer. Anal., 38 (2011), pp. 233–257.

17. S. KINDERMANN AND K. RAIK, *A simplified L-curve method as error estimator*, Electron. Trans. Numer. Anal., 53 (2020), pp. 217–238.

18. S. LU, S. V. PEREVERZEV, AND U. TAUTENHAHN, *Dual regularized total least squares and multi-parameter regularization*, Comput. Methods Appl. Math., 8 (2008), pp. 253–262.

19. V. A. MOROZOV, *Methods for Solving Incorrectly Posed Problems*, Springer, New York, 1984.

20. F. NATTERER, *Regularization of ill-posed problems by projection methods*, Numer. Math., 28 (1977), pp. 329–341.

21. A. NEUBAUER, *An a posteriori parameter choice for Tikhonov regularization in the presence of modeling error*, Appl. Numer. Math., 4 (1988), pp. 507–519.

22. C. C. PAIGE AND M. A. SAUNDERS, *LSQR: An algorithm for sparse linear equations and sparse least squares*, ACM. Trans. Math. Software, 8 (1982), pp. 42–71.

23. R. RAMLAU AND L. REICHEL, *Error estimates for Arnoldi-Tikhonov regularization for ill-posed operator equations*, Inverse Problems, 35 (2019), Art. 055002.

24. L. REICHEL AND G. RODRIGUEZ, *Old and new parameter choice rules for discrete ill-posed problems*, Numer. Algorithms, 63 (2013), pp. 65–87.

25. C. B. SHAW, JR, *Improvements of the resolution of an instrument by numerical solution of an integral equation*, J. Math. Anal. Appl., 37 (1972), pp. 83–112.

26. A. N. TIKHONOV AND V. Y. ARSENIN, *Solutions of Ill-Posed Problems*, Winston, Washington, DC, 1977.

27. G. M. WING, *A Primer on Integral Equations of the First Kind: The Problem of Deconvolution and Unfolding*, SIAM, Philadelphia, 1991.